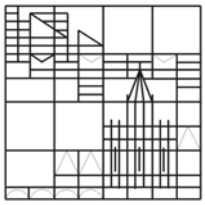

Konstanz University

Acyl-CoA Dehydrogenases:

Characterization of the New Member Isobutyryl-CoA Dehydrogenase, Genetic Defects and Correlation to Thermal Unfolding.

Dissertation submitted to

Department of Biology, Konstanz University, Germany.

For the degree of
Doctor of Natural Sciences

By

M.Sc. Nasser El-Din Ibrahim

Tag der mündlichen Prüfung: 28th of October, 2003
1- Referent: Prof. Dr. Sandro Ghisla
2- Referent: Prof. Dr. Peter Macheroux

ACADs	Acyl-CoA dehydrogenases
ATP	Adenosine triphosphate
A282V	Alanine (number 282) to Valine i3VD mutation
BCA	Bicinchoninic acid
BCAA	Branched-chain amino acids
BCAT	Branched-chain amino-acid transaminase
BCKD	Branched-chain α–ketoacid dehydrogenase
bp	Base-pair
BSA	Bovine serum albumn
CD	Circular dichorism
cDNA	Complementary deoxyribonucleic acid
CPF-CoA	Cyclopropylformylyl-CoA
CPT I	Carnitine palmitoyl transferase I
CT	Charge transfer
DTNB	Ellman´s reagent or 5,5´-DiThiobis(2-Nitrobenzoic acid)
DTT	Cleland´s reagent or DiThioThreitol
2-ECH	2-Enoyl-CoA hydratase
EDTA	Ethylene diamine tetraacetic acid
ETF	Electron transfer flavoprotein
ETF-QO	ETF:coenzyme Q oxidoreductase
FAD	Flavin adnine dinucleotides
FPLC	Fast protein liquid chromatography
GCD	General acyl-CoA dehydrogenase
HIBA	3-Hydroxyisobutyrate
3-HOAD	3-Hydroxyacyl-CoA dehydrogenase
HPLC	High performance liquid chromatography
HRP	anti-Rabbit Horseradish peroxidase
iBD	Isobutyryl-CoA dehydrogenase
IEF	Isoelectric focusing
IPTG	Isopropyl-β-D-Thiogalactopyranoside
i2VD	2-Methylbutyryl-CoA dehy.(2MBDH) or iso2valeryl-CoA dehy.
i3VD	Isovaleryl-CoA dehydrogenase
3-KAT	3-Oxoacyl-CoA thiolase
K304E	Lysine (number 304) to Glutamic MCAD mutation
K_d	Dissociation constant
$K_{d,\ app}$	Apparent dissociation constant
KDa	Kilo Dalton
K_m	Michaelis-Menten constant
KPi	Potassium phosphate buffer
K_U	Equilibrium constant of unfolding reaction
LB	Luria Bertani medium
LCAD	Long-chain acyl-CoA dehydrogenase
LCHAD	Long-chain 3-hydroxyacyl-CoA dehydrogenase
LHYD	Long-chain enoyl-CoA hydratase
LKAT	Long-chain 3-ketoacyl-CoA thiolase
MALDI-TOF	Matrix-assisted Laser desorption/ionization time-of-flight

MCAD	Medium-chain acyl-CoA dehydrogenase
MCPA-CoA	Methylenecyclopropylacetyl-CoA
MKAT	Medium-chain 3-ketoacyl-CoA thiolayase
M/SCHAD	Medium- short-chain L-3-hydroxyacyl-CoA dehydrogenase
MW	Molecular weight
N and U	Native and unfolded protein states
NADH	Nicotine adnine dinucleotides hydrogen
NEM	N-ethylmaleimide
O_2	Molecular oxygen
OD	Optical density
pI	Isoelectric point
R382L	Arginine (number 382) to Leucine IVD mutation
rpm	Revolution per minute
RT	Room temperature
S	Substrate concentration
SBCADH	Short/branched chain acyl-CoA dehydrogenase
SCAD	Short-chain acyl-CoA dehydrogenase
SDS	Sodium dedocyl sulfate
SDS-PAGE	Sodium dedocyl sulfate-polyacrylamide gel electrophoresis
SKAT	Short-chain 3-ketoacyl-CoA thiolyase
T	Tempertaure
T168A	Therione (number 168) to Alanine MCAD mutation
TFP	Trifunctional protein
THF	Tetrahydrofuran
Tm	Midpoint transition
tRNA	Transfer ribonucleic acid
UV-VIS	Ultraviolet and Visible light
V342A	Valine (number 342) to Alanine IVD mutation
VLCAD	Very long-chain acyl-CoA dehydrogenase
V_{max}	Maximum velocity
Wt	Wild type
ε	Extenction coefficient
λ	Wavelength

1 Introduction

1.1 *General Metabolism*

Living organisms require a continual source of energy. This energy is needed for different kinds of processes such as the mechanical work of muscles, active transport of important molecules and biosynthesis of macromolecules. Energy supplied to these processes is in the form of ATP, adenosine triphosphate, a molecule with an energy-rich bond, which is normally found in active form in complex with Mg^{2+} or Mn^{2+} ions. Extraction of energy, in other words ATP production, takes place via energy transformation from one form to another in a process called "energy metabolism". Fatty acid β-oxidation and amino acids degradation are examples of energy producing processes.

1.2 *Fatty Acid β-Oxidation*

The β-oxidation is the major process by which fatty acids are oxidized to provide a major source of energy for heart and skeletal muscles (1) and peripheral tissues, e.g. skeletal muscles, gain access to the lipid energy reserves stored in adipose tissue through three stages of processing. First, the lipid must be transported from the adipose tissue. Triglycerides are degraded to free fatty acids and glycerol, which are released from the adipose tissue and transported to the energy-requiring tissues in a process called lipolysis (2). Lipolysis is regulated by epinephrine, norepinephrine, glucagon and adrenocorticotropic hormones where they induce lipolysis by binding to special receptors. Binding hormones to the receptors increase cAMP inside the cells and subsequently induce lipolysis. On the other hand, when insulin binds to its receptor, it inhibits lipolysis.

At the outer mitochondrial membrane free fatty acids are activated to acyl-CoA esters by the ATP-dependent acyl-CoA synthetase. If intracellular levels of malonyl-CoA decrease in response to fasting, the activity of carnitine palmitoyl transferase I (CPT I) is upregulated and increase the import of the acyl-CoA into the mitochondrial membrane (3). It is important to mention that the cytoskeleton also has a role in the regulation of the CPT I activity (4). It was found that activation of $Ca2^{+}$–CM-PKII ($Ca2^{+}$–calmodulin-dependent protein kinase II) or AMPK (AMP-activated protein

kinase) increases the phosphorylation of cytokeratins 8 and 18 (intermediate filaments of the cytoskeleton) and so it is disrupting the cytoskeleton intermediate filaments. As a consequence, inhibitory interactions between the cytoskeleton and mitochondrial components are lost, allowing more activity for CPT-I and ketogenesis. The exact mechanisms and interactions between mitochondria and cytoskeleton are not known yet (4).

This induces the CPT I reaction toward the formation of acyl-carnitine from acyl-CoA and free carnitine. The acyl-carnitine is now ready to cross the inner mitochondrial membrane by carnitine:acyl-carnitine translocase (CACT) (5). Inside the mitochondrial matrix, the acyl-CoA is formed again by the CPTII enzyme through a reaction of acyl-carnitine with free CoA (6) (Figure1).

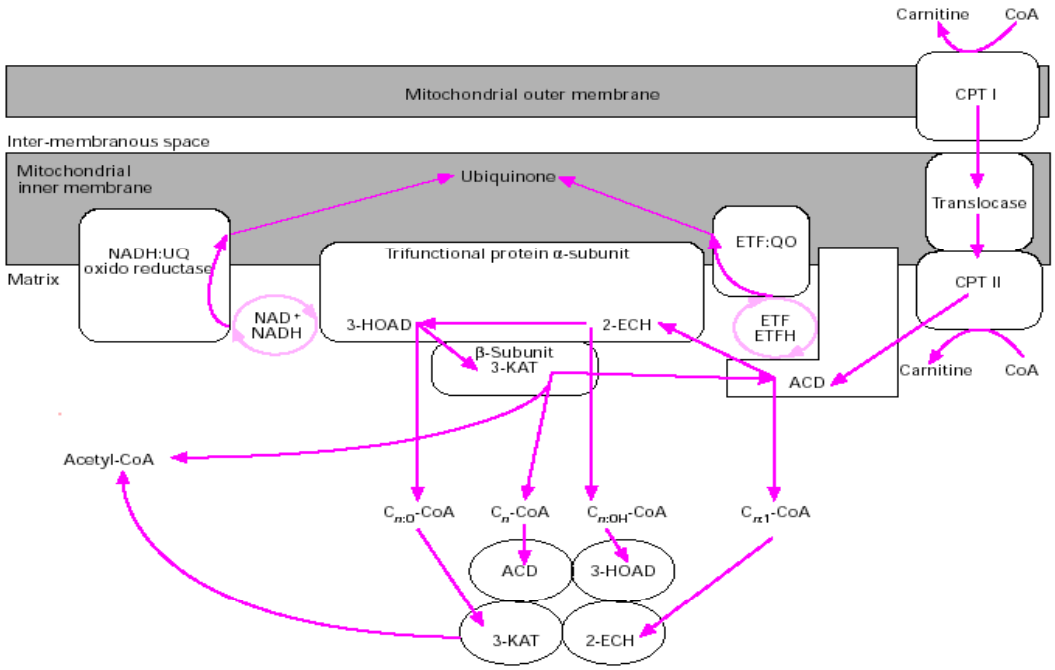

Figure 1. A model for internalization of the fatty acid into the mammalian mitochondria for β-oxidation. C*n*, refers to number of carbon atoms; 2,3-enoyl-CoA esters are indicated by the C*n*:1; 3-hydroxyacyl-CoA esters are indicated by the C*n*:OH and 3-oxoacyl-CoA esters by the C*n*:O. 2-ECH refers to 2-enoyl-CoA hydratase; 3-HOAD refers to 3-hydroxyacyl-CoA dehydrogenase; 3-KAT refers to 3-oxoacyl-CoA thiolase. (From ref. 9).

Medium- and short-chain fatty acids ($C_{12}\geq$) import into the mitochondria independently of the carnitine shuttle. It was proposed that they are activated within the mitochondrial matrix by different acyl-CoA synthetases (7).

The β-oxidation takes place in four steps: oxidation by FAD-dependent acyl-CoA dehydrogenases (ACADs), hydration by enoyl-CoA hydratases, oxidation by NAD^+-dependent enzymes L-3-hydroxyacyl CoA dehydrogenase and thiolysis by β-ketothiolase. Each cycle of β-oxidation produces acetyl-CoA, $FADH_2$, NADH and the original acyl-CoA is shorted by two carbons.

The ACADs include VLCAD, LCAD, MCAD and SCAD. The main difference between them is the preferred length of the substrate. In addition to this family there is a second family that catalyzes the β-oxidation of the substrates that originate from amino acids, which are iBD, i3VD, and i2VD. This to be discussed below. VLCAD is responsible for the reduction across the 2,3 position of the acyl-CoA of C_{12}-C_{24} length (8). Recently, a new gene called ACAD-9 was isolated from a human dendritic cells cDNA library. It has a 65% similarity to human VLCAD (9).

Its electrons arising in the β-oxidation reaction are transferred via electron transfer flavoprotein (ETF) to ETF:coenzyme Q oxidoreductase (ETF-QO) and ultimately to the oxidative phosphorylation pathway from which energy of oxidation is derived (10).While LCAD is responsible for the reduction of the acyl-CoA of C_8-C_{20} length, C_4-C_{12} for MCAD and C_4-C_6 for SCAD. The second difference is that the VLCAD is a homodimer membrane-bound enzyme, while LCAD, MCAD and SCAD are homotetramers and found in the mitochondrial matrix (11) (Figure 2).

The second reaction of β–oxidation involves hydration of the double bond in the 2,3 position to yield a stereo-specific L-3-hydroxyacyl-CoA species. There are two enzymes able to carry out this reaction. The first is long-chain enoyl-CoA hydratase (LHYD) that is specific for hydrating long-chain species. It is a part of a membrane-associated trifunctional enzyme complex called mitochondrial trifunctional protein (TFP). TFP is a heterooctamer of $\alpha_4\beta_4$ subunits. The α subunit contains the LHYD activity and long-chain 3-hydroxyacyl-CoA dehydrogenase (LCHAD). The β subunit has long-chain 3-ketoacyl-CoA thiolase (LKAT) activity (12,13). The second enzyme is crotonase or short-chain enoyl-CoA hydratase. It is specific for the hydration of medium- and short-chain enoyl-CoA (14).

The third step of β-oxidation is the reduction at L-3-hydroxy position to yield a 3-ketoacyl-CoA species. LCHAD is part of the TFP in this step in the reduction of long-

chain species. Medium- and short-chain species reduced by another enzyme, Medium-short-chain L-3-hydroxyacyl-CoA dehydrogenase (M/SCHAD), which is a homodimer mitochondrial matrix soluble enzyme (15).

The fourth, and final step in β-oxidation is the cleaving of the 3-ketoacyl-CoA to yield acetyl-CoA and a two-chain-shortened acyl-CoA. For long-chain species cleavage catalyzed by LKAT that is, again, a part of the TFP complex. However medium-chain 3-ketoacyl-CoA cleave by the medium-chain 3-ketoacyl-CoA thiolase (MKAT) (16), and short-chain 3-ketoacyl-CoA thiolase (SKAT) for short-chain 3-ketoacyl-CoA and is involved in isoleucine catabolism (7).

1.3 *Amino Acid Degradation*

Protein degradation is a vital physiological process by which the cell can control many other processes, e.g. gene transcription, cell cycle and antigen processing (17). Any unneeded free amino acids are degraded for ATP production.

The first step of the amino acid degradation is the deamination of the amino acid into ammonia and α–ketoacids. Ammonia is directed to the urea cycle for removal. The α–ketoacids are metabolized and carbon skeletons can enter metabolic pathways as precursors to glucose or citric acid cycle intermediates, according to the carbon skeleton of the amino acid (Figure 3).

Branched-chain amino acids (BCAA) catabolism

BCAA are essential amino acids, they include leucine, isoleucine and valine. BCAA are transported into cells by a number of Na^+-dependent and Na^+-independent carriers with overlapping specificity. The system L carrier appears to mediate most of their transport (18). The first step in BSAA catabolism is the reversible transamination to form the corresponding α–ketoacids, α–ketoisocaproate, α–keto-β-methylvalerate and α–ketoisovalerate. This reaction is catalyzed by branched-chain amino-acid transaminase (BCAT). The second step is the oxidative decarboxylation of the α–ketoacids by mitochondrial branched-chain α–ketoacid dehydrogenase (BCKD). BCAT is present at low levels in the liver compared to extra hepatic tissues like muscle (19), while BCKD is present mainly in the liver (20).

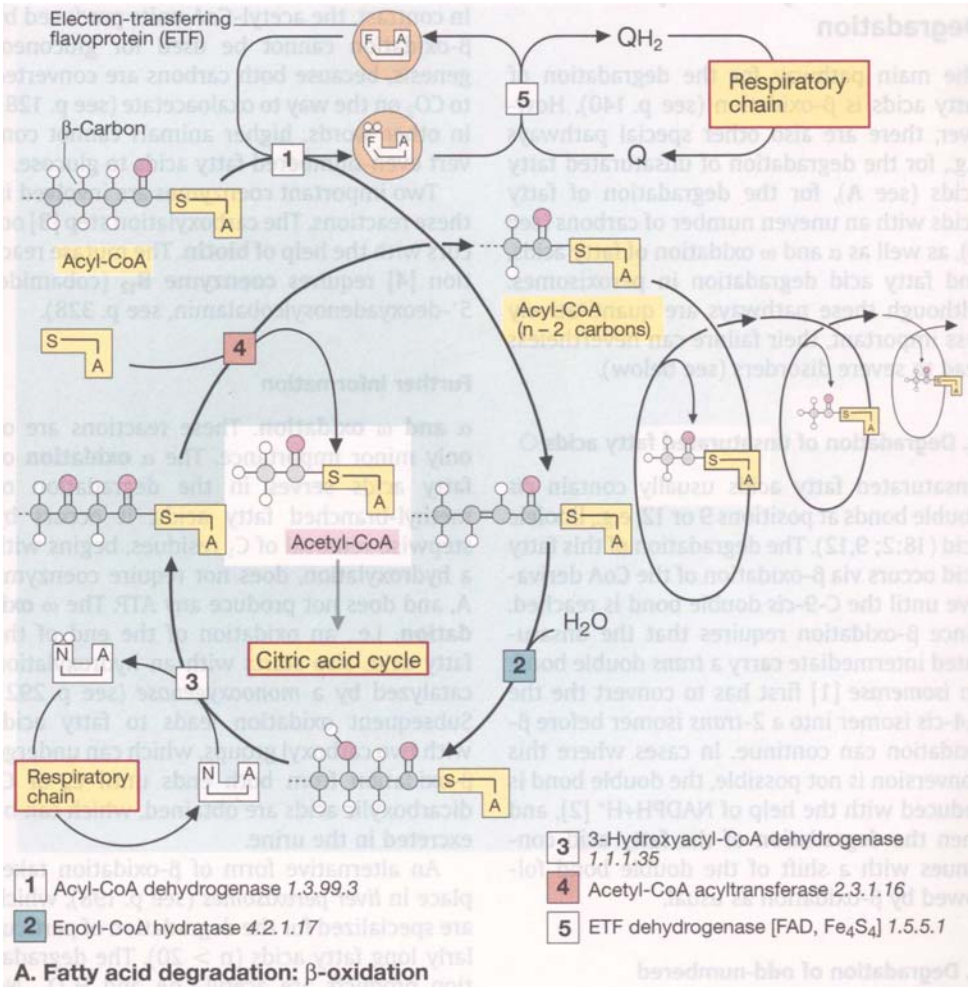

Figure 2. A model for mammalian mitochondrial β-oxidation.
The first step of the pathway is the oxidation of the activated fatty acid by dehydrogenases enzymes [1]. This generates a double bond and two hydrogen atoms that are transferred to ETF and then to the respiratory chain by a reaction catalyzed by ETF dehydrogenase [5]. The water molecule is added to the resultant double bond by the hydratase enzyme [2]. A further dehydration step, the reaction catalyzed by 3-hydroxy-acylCoA dehydrogenase yields a carbonyl group [3]. The two hydrogen atoms are passed to the respiratory chain. The 3-carbonyl-acyl-CoA is then hydrolyzed by the acyl transferase enzyme [4] to yield acetyl-CoA. The latter goes into the citric acid cycle and the acyl-CoA is shortened by two carbons.
(From: Color Atlas of Biochemistry, by Koolman and Röhm).

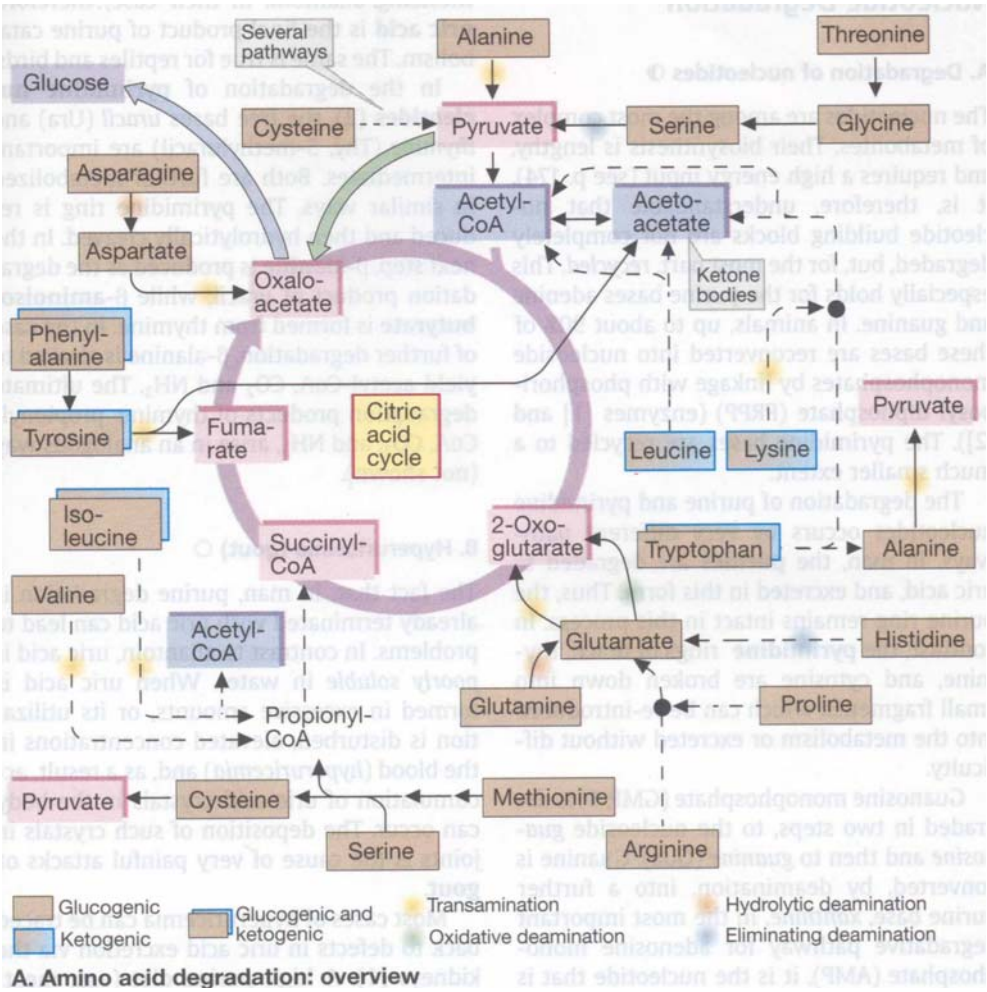

Figure 3. Amino acid degradation overview.
The carbon skeleton of the 20 amino acids yield 7 different degradation products. Five of them (2-Oxoglutarate, succinyl-CoA, fumarate, oxoaloacetate and pyruvate) are precursors of gluconeogensis (can be transformed to glucose) and so the original amino acids are called gluconeogenic. The first four products are intermediates in the citric acid cycle, while pyruvate is converted to oxoaloacetate by pyruvate carboxylase. The other two degradation products, acetoacetate and acetyl-CoA can not be converted into glucose but can form ketone bodies, fatty acids and isoprenoids and so the original amino acids are called ketongenic amino acid. All amino acids are gluconeogenic except lysine and leucine. Phenylalanine, tyrosine, tryptophane and isoleucine are both gluconeogenic and ketogenic. The removal of the amino group is carried out by transamination to the urea cycle or to the 2-oxoglutarate by oxidative deamination. Asparagine and glutamine loose the amino group of the amide group by hydrolytic deamination while serine and pyruvate lose it by eliminating deamination.
(From: Color Atlas of Biochemistry, By Koolman and Röhm).

The catabolism of valine differs from that of other BCAA (leucine and isoleucine) in that 3-hydroxyisobutyrate (HIBA) is formed during its catabolism. This is unique because it is not esterified to CoA. HIBA is produced in the hydrolytic reaction catalyzed by a special enzyme, 3-hydroxyisobutyrate hydrolase (21). The HIBA is reversibly oxidized by 3-hydroxyisobutyrate dehydrogenase (22).
The ACADs, which are responsible for the β-oxidation of the acyl-CoA from the carbon skeleton of the BCAA, include iBD, i3VD and i2VD (Figure 4).

1.4 *Disorders of Mitochondrial β-oxidation*.

Fatty acid oxidation disorders have two pathological consequences. One is the result of energy deficiency and shortage of substrates for gluconeogensis (energy production) due to reduction of the flux through the fatty acid oxidation pathway. The second is the toxic effect of intermediate metabolites that accumulate due to enzyme deficiency. When there is increased requirement for fatty acid oxidation, as occurs during the periods of infant growth, prolonged fasting or exercise, the demand for energy from fatty acid oxidation and for gluconeogensis cannot be sufficient and at the same time there is a probability of accumulation of toxic metabolites. The net result may be metabolic decompensation and clinical disease.

But there is overlapping substrate specificity between fatty acid oxidation enzymes, e.g., LCAD catalyzes the dehydrogenation of substrates of chain-length C_8-C_{20} and C_4-C_{12} for MCAD. This overlapping may modify the pathological effects of a given enzyme defect. Additionally, modulation may be exerted by alternative metabolic pathways, which can detoxify the accumulated metabolites (23).
These alternative pathways result in the formation of metabolic products observed in blood and/or urine such as amide conjugates with glycine or carnitine and synthesis of dicarboxylic acids. The relative amounts of resultant glycine- and carnitine-conjugates as well as dicarboxylic acids rely on affinities of detoxifying enzymes for the various accumulated substrates or, that is mean, how fast the detoxifying enzymes can get ride of these accumulated substrates. Therefore, and also due to the inter-individual variation in the capacity of various detoxification pathways, the modulation of an

enzyme defect may vary remarkably between diseases and between patients with the diseases (23).

Many genetic defects have been reported for the mitochondrial fatty acid β-oxidation. These include defects in VLCAD, LCAD, MCAD and SCAD (23, 24, 25, 26).
VLCAD deficiency patients can be subdivided into three groups. Group 1 comprises very young infants less than one year of age and many of whom die with severe cardiac and hepatic symptoms. The main accumulated metabolite is tetradecanoyl-carnitine. Group 2 comprises older children, aged 1-13 years and showing hypoketotic hypoglycemia without cardiomyopathy. The principal accumulated metabolite is dodecanoyl-carnitine. Group 3 comprises adults with muscle weakness and pain without cardiac or hepatic symptoms. For LCAD, the symptoms range from dilated cadriomyopathy and fasting hypoglycemia to sudden death.
The clinical features of the SCAD deficiency range from hypoglycemia and vomiting to hypotonia and developmental delay. MCAD and its deficiency, along with that for i3VD and iBD, are discussed in more details below.

Human Medium-Chain Acyl-CoA dehydrogenase (MCAD) and its deficiency
MCAD deficiency is the best known and still the most frequently encountered fatty acid oxidation defect. The frequency varies from one region to another, with north-central Europe estimated at 1:13,000 in the Netherlands and England; 1:30,000 in Denmark, Germany and Poland; 1:300,000 in southern Europe. In the USA it is estimated to be at 1:15,000. MCAD deficiency is a disease that is prevalent in Caucasians, with a carrier frequency for the common K304E mutation of the MCAD gene of about 1:40. The overall frequency of the mutation has been estimated to be in the range of 1:6,500-1:17,000 (27). Another example of MCAD mutation is the T168A mutation, where the amino acid exchange is located in the active site of the enzyme. The threonine is located in contact with the FAD cofactor and forms a hydrogen bond with the flavin-nitrogen N(5) (28). Patients with MCAD deficiency are regarded as normal at birth even when transient episodes of “benign” hypoglycemia are observed. Later, usually between 3 and 24 months of age, acute decompensation might occur in response to fasting (e.g., weaning the infant from night time feedings) or common

infections (e.g., viral, gastrointestinal or upper respiratory tract infections) associated with reduced food intake and increased energy requirements. Unexpected death during the first metabolic decompensation is common and may occur as late as in adulthood (29). Although metabolic stress may quickly progress to a life-threatening situation, the prognosis is excellent once the diagnosis is established, especially if detected by newborn screening before the onset of symptoms (30). MCAD deficiency is mainly present with liver associated symptoms (hypoketotic hypoglycemia and coma) but muscular and neurological symptoms have been observed in a few cases.

Human Isovaleryl-CoA dehydrogenase (i3VD) and its deficiency

i3VD is the best-studied member of the ACADs subfamily involved in the catabolism of amino acids (31), its biochemical properties have been addressed, and its 3D-structure is known (32). Also, in i3VD's case several mutants involving amino acid replacements have been discovered in humans that lead to isovaleric academia, which can present with a widely variable spectrum of symptoms and some of the defects seem partly related to protein instability (33). The least functionally defective of the i3VD mutants are A282V, V342A, and R382L, with apparent residual activity below 20% compared to wild type (33).

1.5 References

1- **Felig, P., and Wahren, J.** (1975) Fuel homeostasis in exercise. *N. Engl. J. Med*. **293**:1078-84.

2- **Berk, P. D., and Stump, D. D.** (1999) Mechanisms of cellular uptake of long chain free fatty acids. *Mol. Cell. Biochem*. **192**:17–31.

3- **Britton, C. H., Schultz, R. A., Zhang, B., Esser, V., Foster, D. W., and McGarry, J. D. (**1995) Human liver mitochondrial carnitine palmitoyl- transferase I: characterization of its cDNA and chromosomal localization and partial analysis of the gene. *Proc. Natl. Acad. Sci. USA.* **92**:1984–88.

4- **Guzmán, M., Velasco, G., and Geelen, M. J. H.** (2000) Do cytoskeleton components control fatty acid translocation into liver mitochondria.*TEM*.**11**:49-53.

5- **Huizing, M., Iacobazzi, V., Ijlst, L., Savelkoul, P., Ruitenbeek, W., van den Heuvel, L., Indiveri, C., Smeitink, J., Trijbels, F., Wanders, R., and Palmieri, F.** (1997) Cloning of the human carnitine-acylcarnitine carrier cDNA and identification of the molecular defect in a patient. *Am. J. Hum. Genet*. **61**:1239–45.

6- **Finocchiaro, G., Taroni, F., Rocchi, M., Martin, A. L., Colombo, I., Tarelli, G. T., and DiDonato, S.** (1991) cDNA cloning, sequence analysis, and chromosomal localization of the gene for human carnitine palmitoyl- transferase. *Proc. Natl. Acad. Sci. USA.* **88**:661–65.

7- **Rinaldo, P., and Matern, D.** (2002) Fatty acid oxidation disorders. *Annu. Rev. Physiol*. **64**:477-502.

8- **Izai, K., Uchida, Y., Orii, T., Yamamoto, S., and Hashimoto, T.** (1992) Novel fatty acid β-oxidation enzymes in rat liver mitochondria.I: purification and properties

of verylong-chain acyl coenzyme A dehydrogenase. *J. Biol. Chem*. **267**:1027–33.

9- Zhang, J., Zhang, W., Zou, D., Chen, G., Wan, T., Zhang, M., and Cao, X. **(2002) Cloning and functional characterization of ACAD-9, a novel member of human acyl-CoA dehydrogenase family. *Biochem. Biophys. Res. Commun.*** 297**:1033-1042.**

10- **Eaton, S., Bartlett, K., and Pourfarzam, M.** (1996) Mammalian mitochondrial β-oxidation. *Biochem. J.* **320**:345–57.

11- **Ikeda, Y., Okamura-Ikeda, K., and Tanaka, K.** (1985) Purification and characterization of short-chain, medium-chain, and long-chain acyl-CoA dehydrogenases from rat liver mitochondria. Isolation of the holo- and apoenzymes and conversion of the apoenzyme to the holoenzyme. *J. Biol. Chem*. **260**:1311–25.

12- **Uchida, Y., Izai, K., Orii, T., and Hashimoto, T.** (1992) Novel fatty acid β-oxidation enzymes in rat liver mitochondria. II: purification and properties of enoyl-CoA hydratase-3-hydroxyacyl-CoA dehydrogenase-3-ketoacyl-CoA thiolase trifunctional protein. *J. Biol. Chem*. **267**:1034–41.

13- **Carpenter, K., Pollitt, R. J., and Middleton, B.** (1992) Human long-chain 3-hydroxyacyl-CoA dehydrogenase is a multifunctional membrane-bound β-oxidation enzyme of mitochondria. *Biochem. Biophys. Res. Commun.* **183**:443–48.

14- **Kanazawa, M., Ohtake, A., Abe, H., Yamamoto, S., Satoh, Y., Takayanagi, M., Niimi, H., Mori, M., and Hashimoto, T**. (1993) Molecular cloning and sequence analysis of the cDNA for human mitochondrial short-chain enoyl-CoA hydratase. *Enzyme Protein* **47**:9–13.

15- **Kobayashi, A., Jiang, L. L, and Hashimoto, T.** (1996) Two mitochondrial 3-hydroxyacyl- CoA dehydrogenases in bovine liver. *J. Biochem*. **119**:775–82.

16- **Miyazawa, S., Osumi, T., and Hashimoto, T.** (1980) The presence of a new 3-oxoacyl-CoA thiolase in rat liver peroxisomes. *Eur. J. Biochem*. **103**:589–96.

17- **Hochstrasser, M.** (1996) Ubiquitin-dependent protein degradation. *Annu. Rev. Genet.* **30**:405–39.

18- **Shotwell, M. A., Kilberg, M. S., and Oxender, D. L**. (1983) The regulation of neutral amino acid transport in mammalian cells. *Biochim Biophys Acta*. **737**:267-84.

19- **Shinnick, F. L., and Harper, A. E.** (1976) Branched-chain amino acid oxidation by isolated rat tissue preparations. *Biochim Biophys Acta*. **437**:477-86.

20- **Wohlhueter, R. M., and Harper, A. E.** (1970) Coinduction of rat liver branched chain alpha-keto acid dehydrogenase activities. *J. Biol. Chem*. **245**:2391-401.

21- **Hawes, J. W, Jaskiewicz, J., Shimomura, Y., Huang, B., Bunting, J., Harper, E. T., and Harris, R. A.** (1996) Primary structure and tissue-specific expression of human beta-hydroxyisobutyryl-coenzyme A hydrolase. *J. Biol Chem.* **271**:26430-4.

22- **Hawes, J. W., Harper, E. T., Crabb, D. W., and Harris, R. A.** (1996) Structural and mechanistic similarities of 6-phosphogluconate and 3-hydroxy isobutyrate dehydrogenases reveal a new enzyme family, the 3-hydroxyacid dehydrogenases. *FEBS Lett*. **389**:263-7.

23- Gregersen, N., Andresen, B. S., Corydon, M. J., Corydon, T. J., Olsen, R. K., Bolund, L., and Bross, P. **(2001) Mutaion analysis in mitochondrial fatty acid oxidation defects: Exemplified by acyl-CoA dehydrogenase deficiencies, with special**
focus on genotype-phenotype relationship. Hum. Mutat. 18**:169-89.**

24- **Hale, D. E., Stanley, C. A., and Coates, P. M.** (1990) The long chain acyl-CoA dehydrogenase deficiency. *Progr. Clin. Biol. Res*. **321**:411–18.

25- **Stanley, C. A., Hale, D. E., Coates, P. M., Hall, C. L., Corkey, B. E., Yang, W., Kelley, R. I., Gonzales, E. L., Williamson, J. R., and Baker, L.** (1983) Medium-chain acyl-CoA dehydrogenase deficiency in children with non-ketotic hypoglycemia and low carnitine levels. *Pediatr. Res*. **17**: 877–84.

26- **Coates, P. M., Hale, D. E., Finocchiaro, G., Tanaka, K., and Winter, S. C.** (1988) Genetic deficiency of short-chain acyl-coenzyme A dehydrogenase in cultured fibroblasts from a patient with muscle carnitine deficiency and severe skeletal muscle weakness. *J. Clin. Invest*. **81**:171–75.

27- Matern, D., and Rinaldo, P. **(2000) Medium chain acyl-coenzyme A (MCAD) deficiency. In GeneClinics: Medical Genetics Knowledge Base [database online]. Univ.Washington, Seattle. http://www.geneclinics.org/profiles/mcad.**

28- **Küchler, B., Abdel-Ghany, A. G., Bross, P., Nandy, A., Rasched, I., and Ghisla, S.** (1999) Biochemical characterization of a variant human medium-chain acyl-coA dehydrogenase with a disease-associated mutation localized in the active site. *Biochem J*. **337**:225-30.

29- **Raymond, K., Bale, A. E., Barnes, C. A., and Rinaldo, P**. (1999) Sudden adult death and medium-chain acyl-CoA dehydrogenase deficiency. *Genet. Med***. 1**:293 –94.

30- **Chace, D. H., Hillman, S. L., Van Hove, J. L., and Naylor, E. W.** 1(997) Rapid diagnosis of MCAD deficiency: quantitatively analysis of octanoylcarnitine and other acylcarnitines in newborn blood spots by tandem mass spectro- metry.
Clin. Chem. **43**:2106–13.

31- **Tanaka, K., Ikeda, Y., Matsubara, Y. and Hyman, D.** (1987) Molecular basis of isovaleric academia and medium chain acyl-CoA dehydrogens deficiency.
Enzyme **38**: 91-107.

32- **Tiffany, K. A., Roberts, D. L., Wang, M., Paschke, R., Mohsen, A. A., Vockley, J., and Kim, J. J. P.** (1997) Structure of human isovaleryl-CoA dehydro- genase at 2.6 A resolution: structural basis for substrate specificity. *Biochemistry*. **36**:8455-64.

33- **Mohsen, A. A., Andreson, B. D., Volchenboum, S. L., Battaile, K. P., Tiffany, K., Roberts, D., Kim, J., and Vockley, J.** (1998) Characterization of molecular defects in Isovaleryl-CoA dehydrogense in patients with isovaleric academia. *Biochemistry* **37**:10325-35.

2 Chapter Ia

Human Isobutyryl-CoA Dehydrogenase: A New member of the Acyl-CoA Dehydrogenase Family. Identification and Deficiency in Humans.

2.1 Summary

The acyl-CoA dehydrogenases (ACADs) are a family of related enzymes that catalyze the a,ß-dehydrogenation of acyl-CoA esters. Two homologues active in branched chain amino acid metabolism have previously been identified. We have used expression in *E. coli* to produce a previously uncharacterized ACAD-like sequence (*ACAD8*) and define its substrate specificity. Purified recombinant enzyme had a *k*cat/*K*m of 0.8, 0.23 and 0.04 (mM-1s-1) with isobutyryl-CoA, (S) 2-methyl butyryl-CoA, and n-propionyl-CoA, respectively, as substrates. Thus, this enzyme is an isobutyryl-CoA dehydrogenase. A single patient has previously been described whose fibroblasts exhibit a specific deficit in the oxidation of valine. Amplified *ACAD8* cDNA made from patient fibroblast mRNA was homozygous for a single nucleotide change (905G>A) in the *ACAD8* coding region compared to the sequence from control cells. This encodes an Arg302Gln substitution in the full-length protein (position 280 in the mature protein), a position predicted by molecular modeling to be important in subunit interactions. The mutant enzyme was stable but inactive when expressed in *E. coli*. It was also stable and appropriately targeted to mitochondria, but inactive when expressed in mammalian cells. These data confirm further the presence of a separated ACAD in humans specific to valine catabolism (isobutyryl-CoA dehydrogenase, iBD), along with the first enzymatic and molecular confirmation of a deficiency of this enzyme in a patient.

2.2 Introduction

The acyl-CoA dehydrogenases (EC 1.3.99.3) are a family of nuclear encoded, mitochondrial flavoenzymes that catalyze the a,b-dehydrogenation of acyl-CoA intermediates in the catabolism of fatty acids and branched chain amino acids (1-7). Inherited deficiencies of these enzymes are important causes of human disease (8-10).

Early studies of ACADs isolated from rat liver mitochondria suggested the existence of a single enzyme (called 2-methylbranched chain acyl-CoA dehydrogenase) that could utilize both isobutyryl- and S-2-methylbutyryl-CoAs from the valine and isoleucine pathways, respectively, equally well as substrates (3). More recently, the rat and human cDNAs for this enzyme have been cloned and the gene was named short/branched chain acyl-CoA dehydrogenase (*ACDSB*; see Table 1 for a summary of genetic nomenclature and protein designations) (6,7,11).

Table 1
Genetic loci and common enzyme names for ACADs involved in short and branched chain amino acid catabolism

Genetic Locus	Enzyme Name	Catabolic Pathway
IVD	Isovaleryl-CoA dehydrogenase (i3VD)	Leucine
ACADSB	Short/branchedcchain acyl-CoA dehydrogenase (i2VD) 2-Methylbranched chain acyl-CoA dehydrogenase (i2VD)	Isoleucine
ACAD8	Isobutyryl-CoA dehydrogenase (iBD)	Valine
ACADS	Short chain acyl-CoA dehydrogenase (SCAD)	Mitochondrial fatty acid β-oxidation

Recombinant rat `i2VD` produced in *E. coli*, like its native counterpart, could efficiently utilize both isobutyryl- and 2-methylbutyryl-CoA as substrate. In contrast, the recombinant human enzyme did not efficiently utilize isobutyryl-CoA as substrate, raising the possibility that another ACAD specific to valine metabolism might exist in humans. Two patients with inactivating mutations in the *ACADSB* gene have recently been identified (12,13). In the first of these patients, valine metabolism was shown to be normal, while this was not examined in the second patient. Finally, a patient has been identified in whom metabolic loading studies in fibroblasts revealed decreased oxidation of labeled valine, with an increase in accumulation of isobutyryl carnitine. Metabolism of labeled isoleucine and leucine was normal, and a defect in a valine specific ACAD was proposed (14).

A mapping study of human chromosome 11q25 has identified a novel gene that shares strong homology to other members of the human ACAD gene family (15). Initial studies of *ACAD8* cDNA revealed that the protein expressed in an eukaryotic system had high activity towards both 2-methylbutyryl-CoA and isobutyryl-CoA in crude cellular extracts (13). We now report expression of the cDNA for *ACAD8* in *E. coli*, purification of the recombinant enzyme to homogeneity, and characterization of the kinetic properties and substrate specificity of the purified enzyme. We also report the gene structure of the human *ACAD* gene. Mutation analysis of *ACAD8* from the patient with a proposed defect in valine metabolism revealed a mutation in the *ACAD8* coding region leading to loss of enzymatic activity. Our findings identify *ACAD8* as an isobutyryl-CoA dehydrogenase (iBD) active in valine catabolism, as well as the first patient deficient in this enzyme.

2.3 Materials and methods

2.3.1 Construction of wild type human iBD expression plasmid. PCR primers were designed to amplify the predicted 1182 base pairs of the mature coding region of *ACAD8* cDNA. The 5'-primer consisted of 47 nucleotides including nucleotides 67 to 95 of the precursor coding sequence followed by *EcoRI* (underlined) and *NdeI* (bold) restriction sites (5'-GAC GAT GAA TTC **CAT ATG** CTC GTC CAG ACC GGC CAC CGG AGC TTG AC-3'). The 3'-primer consisted of the last 15 nucleotides of the coding region (stop codon in antisense direction is bolded) followed by a *HindIII* restriction site (underlined) (5'-AAT GAG AAG CTT **CTA** CTA CTC CTG AAG CAG-3'). A human liver Marathon-ready cDNA from Clontech (Palo Alto, CA) was used as template for PCR, which was performed with 30 cycles of annealing 60° C for 30 sec, extension 68° C for 4 min, and denaturing 94° C for 30 sec using the Advantage cDNA PCR Kit with Polymerase Mix (Clontech, Palo Alto, CA). PCR products were purified by electrophoresis on a 1.5 % low melting agarose gel, and the desired DNA band recovered using the QIAquick Gel Extraction Kit 50 (QIAGEN, Valencia, CA). The recovered fragment was digested with *Eco*RI and *Hind*III, and inserted into the prokaryotic expression vector pET-21a (+) (Novagen, Madison, WI). The plasmid containing the mature iBD insert (*pm*IBD) was used for expression in *E. coli*. To construct the variant iBD plasmid, a *Bse*RI and *Nsi*I restriction fragment containing the

iBD patient mutation was substituted into the same sites in the wild type vector. Precursor wild type iBD was expressed in COS-7 cells using a pcDNA3.1(+) vector as previously described (12,13). The patient mutation was introduced into the precursor iBD sequence via the replacement of a *Bsm*I and *Nsi*I fragment with the same fragment containing the patient mutation.

2.3.2 Amplification of *ACAD8* sequences made from fibroblast mRNA.

mRNA was isolated from control and patient cultured fibroblasts using the QuickPrep Micro mRNA Purification Kit (Amersham Pharmacia Biotech, Pistcataway, NJ), and first strand cDNA was synthesized with the First-Strand cDNA Synthesis Kit (Amersham Pharmacia Biotech). *ACAD8* cDNA sequences were amplified by 30 cycles of PCR: 62° C, 4 min, annealing; 72° C, 7 min, extension; and 94° C, 30 sec denaturing. Amplified products were separated and purified as before, and subjected to automated DNA sequencing by the Molecular Biology Core Facility of the Mayo Clinic.

2.3.3 Identification and characterization of the human *ACAD8* gene structure and sequence analysis of patient and control genomic DNA.

tBlast homology searches of the HTGS and GSS databases in GenBank with the predicted amino acid sequence of the human *ACAD8* were used to identify two BAC clones containing part of the human *ACAD8* gene: AC018780 and AP000859. The AP000859 BAC has been mapped to chromosome 11q25, which is consistent with the previous mapping of the human *ACAD8* gene (15). Intron sizes were estimated on the basis of migration in agarose gels of PCR products amplified with primers located in separate exons and from the sequence of AC018780 and AP000859. Primers were designed for PCR amplification of the eleven exons and part of the flanking intron sequences of the human *ACAD8* gene (primer sequences are available on request brage@biobase.dk). Genomic DNA was isolated from cultured fibroblasts or blood samples according to standard methods (16). PCR reactions were performed under standard conditions in an automated Thermal cycler 480 (Perkin Elmer, Norwalk, CT), and the PCR products were subjected to direct bi-directional cycle sequencing as described above.

2.3.4 Expression of wild type and mutant iBD.

*pm*IBD was transformed into *E. coli* host strain BL21(DE3; Novagene, Madison, WI), crude extracts of induced cells were made from 25 ml of cultures grown in 2xYT (31 g/l, BIO 101, Vista, CA) with 80mg/ml ampicillin. Cultures of *E. coli* were grown to mid-log phase (absorbance 550 nm > 0.5), induced by the addition of IPTG to 0.5 mM final concentration, and incubated with shaking at 37°C for 4 hours or overnight. Cells were harvested by centrifugation, and lysed by sonication after treatment with lysozyme as previously described (17-20). For large-scale purification, the wild type and Arg280Gln mutant iBD plasmids were co-expressed with the bacterial chaperonins Gro EL/GroES, grown at 29o C, and harvested after 4 hours induction. Expression in COS-7 cells, immunostaining, and confocal laser microscopy were performed as described (13,21). The presence of iBD protein in prokaryotic and eukaryotic cell extracts was determined through western blotting with iBD specific antisera as previously described (12,13).

2.3.5 Purification of iBD protein.

Wild type iBD protein was purified from induced *E. coli* cultures by DEAE chromatography, fractionation with ammonium sulfate, and chromatography on 10 mm hydroxyapatite as previously described (17-19). To prevent loss of FAD from the enzyme molecule, 20 μM FAD was added to the buffer during elution from the hydroxyapatite column. Free FAD was removed from final sample by filtration on Superdex G- 200 in 50 mM potassium phosphate, pH 7.5, 0.1M KCl.

2.3.6 Enzyme assays. ACAD activity was measured with the anaerobic electron transfer flavoprotein (ETF) reduction assay using an LS50B fluorescence spectrophotometer from Perkin Elmer (Norwalk, CT) with a heated cuvette block set to 32oC as described (22). Final substrate concentration in the assay mixtures was 50 μM. For activity units (U) see (22).

2.3.7 Molecular modeling of iBD structure.

A prediction of the three dimensional structure of iBD was obtained with the Insight II 2000 package of modeling software from Accelrys, Inc. (San Diego, CA) and a Silicon Graphics O2 workstation (Mountain View, CA). Modeling based on the published structures of human isovaleryl-CoA dehydrogenase (`i3VD`), porcine medium chain acyl-CoA dehydrogenase (MCAD), and butyryl-CoA dehydrogenase from *M. elsdenii* (23-26) was performed using the Homology and Modeler modules included with this software as previously described (22). The "Manual Rotomer" option was used to optimize the position of atoms of the side chains of specific amino acid residues and examine the energy minima of the various possible conformations.

2.3.8 Computational protein sequence analysis.

The protein sequence of 22 selected ACADs were identified from different species via a standard BLAST search of the NCBI databases and compared with the human iBD sequence using the MacVector software package version 7.0 with the Clustal W algorithm v 1.4, and distance matrix methods. The multiple sequences were aligned and a phylogenetic tree constructed using the following parameters: Pairwise alignment mode, slow; open gap penalty, 10.0; extend gap penalty, 0.1; delay divergent, 40%; gap distance, 8; and similarity matrix, blosum. Table 2 shows the Genbank accession numbers of protein sequences analyzed.

Table 2
Species of origin and accession numbers of ACADs-like protein sequences

Species name and enzyme	Abbreviations in Figs 5 and 6	Accession number
Arabidopsis thaliana i3VD	IVDH A.t.	CAA73227
Bacillus halodurans iBD	ACDH B.h.1	BAB07517
Bacillus halodurans i2VD	ACDH B.h.2	BAB07518
C. elegans i3VD	IVDH C.e.	T16568
C. elegans *i2VD*	SBCADH C.e.	T15088
Drosophila melanogaster i3VD	IVDH D.m.	AAF50398
Drosophila melanogaster i2VD	SBCADH D.m.	AAF49216
Drosophila melanogaster SCAD	SCADH D.m.	AAF55709
Human iBD	IBDH human	AAF12736
Human i3VD	IVDH human	P26440
Human i2VD	SBCADH human	AAA74424
Human SCAD	SCADH human	P16219
Mouse i3VD	IVDH mouse	AAF35888
Mouse SCAD	SCADH mouse	AAA16714
Mycobacterium tuberculosis iBD	IBDH M.t.	C07825
Pig SCAD	SCADH pig	BAA13964
Pisum sativum SCAD	IVDH pea	CAB55554
Potato i3VD	IVDH potato	CAC08233
Pseudomonas aeruginosa iBD	IBDH P.a.	AAG04135
Pseudomonas aeruginosa i3VD	IVDH P.a.	AAG05403
Rat i3VD	IVDH rat	P12007
Rat i2VD	SBCADH rat	AAB17136
Rat SCAD	SCADH rat	B30605

2.4 Results

The clinical history of the patient studied has previously been reported (14). Briefly, she presented at 2-years of age to first cousin parents of Hispanic origins. She was well for the first one and one-half months of life on breast feeding, then developed feeding intolerance on formula. At 11 months of age she was found to have failure to thrive, a severe carnitine deficiency, and dilated cardiomyopathy. She responded well to carnitine therapy and has been well without episodes of decompensation since. She is now 6 years old with normal growth and development. Metabolic flux studies originally revealed a defect in valine catabolism, and the existence of a valine specific acyl-CoA dehydrogenase was suggested. We hypothesized that the recently identified *ACAD8* might be such an enzyme and that it might be deficient in this patient.

To examine this, we amplified *ACAD8* sequences from control and patient fibroblasts. Amplification of *ACAD8* from cDNA made from control fibroblast mRNA yielded a fragment of 1250 base pairs in size, in good agreement with the size of the predicted precursor form of *ACAD8* (15). Direct DNA sequencing of the amplified product confirmed that the sequence of the PCR product matched that published for *ACAD8* (not shown). In contrast, *ACAD8* sequences amplified from cDNA made from patient fibroblasts revealed a homozygous substitution of a guanine by an adenine residue at position 905 (905G>A) of the precursor coding region (Figure 1). This leads to an Arg302Gln alteration in the precursor, full-length protein, which corresponds to amino acid 280 in the predicted mature protein. To characterize this mutation in genomic DNA, we defined the genomic structure of the human *ACAD8* gene (Table 3; Accession numbers AF260679-AF260689). The human *ACAD8* gene structure was confirmed by PCR and direct sequencing of all exons from genomic DNA from several control samples. Exon 1 is located in AC018780 (Homo sapiens chromosome 11 clone RP11-153c14). Exons 2-11 are located in AP000859 (mapped to 11q25). PCR amplification and sequence analysis of all 11 exons of the *ACAD8* gene from the index patient showed that the 905G>A mutation observed in patient *ACAD8* cDNA was also present in homozygous form in *ACAD8* exon 8 in genomic DNA (not shown). Both parents of the index patient were heterozygous for the 905G>A mutation by sequence analysis of exon 8 amplified from genomic DNA. Sequence analysis of exon 8 amplified from genomic DNA from 59 control individuals (118 alleles) showed that the 905 G>A alteration was not present, though the samples were not matched for ethnic origin.

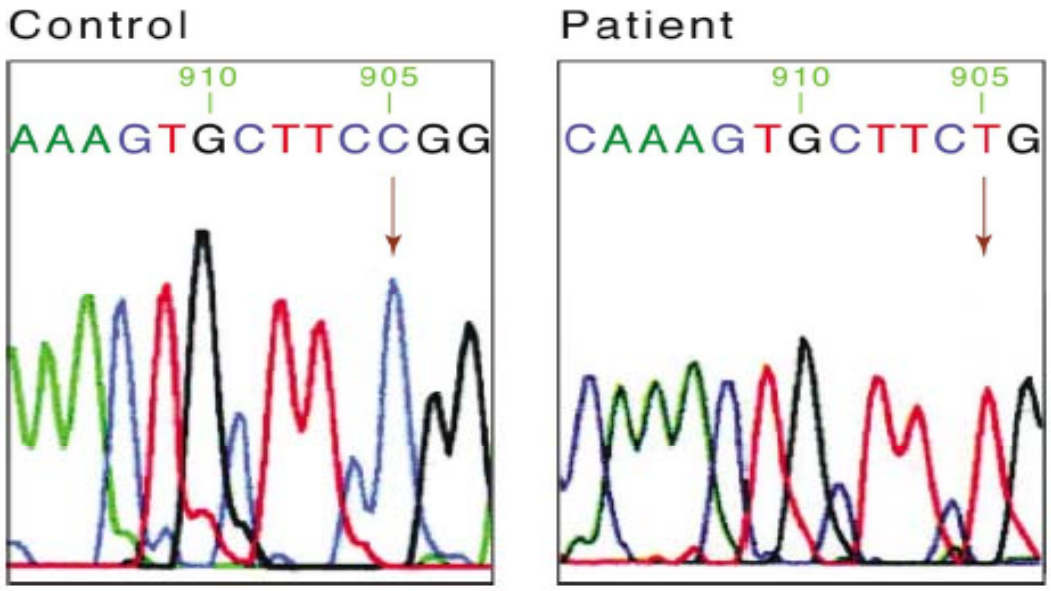

Figure 1. DNA sequencing of control (A) and patient (B) iBD cDNA. A homozygous nucleotide substitution (905 G>A) was identified in the patient cDNA by direct sequencing of sequences amplified from patient fibroblasts. The chromatogram shows a sequence obtained in the reverse direction. This predicts an Arg280Gln alteration in the mature iBD subunit (position 302 of the precursor protein). Sequencing of genomic DNA from the patient confirmed that the patient was homozygous for the mutation (not shown).

Table 3
Organization of the human *ACAD8* gene

Intron 3′ splice site	Exon[a]	5′ Exon sequence	Exon size	3′ Exon sequence	Intron 5′ splice site	Intron size
	Exon 1	([b])		*TGCATCGACC*	gtaaggatct	ND[c]
ctgcccacag	Exon 2	CTTCCATGGG	111	GGACCAGAAG	gtaggcgttt	439
ttgtacatag	Exon 3	GAGCTGTTCC	170	GCATCCACAA	gtgagtgccc	ND[c]
tacctatcag	Exon 4	CATGTGTGCC	120	ACTGAACCAG	gtgaatttgc	383
ccctcctcag	Exon 5	GAAGTGGGAG	77	TGGCTCCAAG	gtactagcgt	51
accccacag	Exon 6	GCCTTCATCA	138	GGAGAAAAAG	gtgagtggct	1238
ttttgccag	Exon 7	GTGGGGTGGA	136	ATCAATATTG	gtgagatacg	95
tcccctctag	Exon 8	CTTCCTGCTC	98	CAGTAACCAG	gtaacctctg	351
tgtgctgcag	Exon 9	TACTTGCAAT	153	ATGCTTTGCC	gtaagtgatt	629
ctcccctgcag	Exon 10	ATCTGCAACC	103	ATTCTAGAAG	gtaaaaattg	2225
cctcttacag	Exon 11	GTAGCAATGA	943	Poly(A) addition site		
Consensus Splice signal						
YYYYYYYYYNAG		G		AG	GTRAGT	

[a] The start position of each exon is indicated relative to the corresponding position in the cDNA sequence. Intron and exon sizes are indicated, and 10 bp of the exon and intron sequences at each junction are presented. Exon 1 is located in AC018780 (*Homo sapiens* chromosome 11 clone RP11-153c14). Exons 2–11 are located in AP000859, mapped to 11q25. The sequence data have been submitted to the GenBank database (Accession Nos. AF260668 –AF260678).

[b] Transcription initiation site not determined.

[c] Not determined.

Extracts from COS-7 cells expressing *ACAD8* were previously reported to have nearly equal activity using isobutyryl-CoA and 2-methylbutyryl-CoA as substrates at high concentrations (12,13). To characterize better the substrate specificity of ACAD8 and the effect of the amino acid substitution on its activity, the predicted mature coding region of *ACAD8* (beginning with amino acid residue Leu23 of the precursor as predicted by consensus processing signals for mitochondrial precursor proteins) was amplified via PCR and cloned into a prokaryotic expression vector. Expression of the insert was induced with IPTG following transformation into *E. coli*, crude cellular extracts were prepared, and the ACAD activity of the extracts was measured in triplicate with a variety of acyl-CoA substrates using the sensitive and highly specific anaerobic ETF fluorescence reduction assay. Extracts from cells containing the wild type *ACAD8* sequence after 4 hours of induction showed the highest activity with isobutyryl-CoA (149 ± 37 mU/mg protein). Activity of the same quantity of crude extract measured with (R/S) 2-methyl butyryl-CoA and (S) 2-methyl butyryl-CoA as substrates was 63 ± 2 and 69 ± 15 mU/mg protein, respectively. No activity was detectable in the cellular extract when *n*-butyryl-CoA, *n*valeryl-CoA, or isovaleryl-CoA were used as substrates. The recombinant enzyme was purified to >95% homogeneity (Figure 2A) and kinetic parameters determined using the ETF fluorescence reduction assay. Results (Table 4) confirm that expressed ACAD8 protein has maximal activity towards isobutyryl-CoA and thus we name this enzyme isobutyryl-CoA dehydrogenase (iBD).

Table 4
Comparison of the kinetic parameters of purified wild type iBD measured with different substrates and the ETF fluorescence reduction assay

Substrate	K_m (μM)	k_{cat} (s^{-1})	Tetramer catalytic efficiency (μM^{-1} s^{-1})
Isobutyryl-CoA	2.6 ± 0.7[a] (*N* = 24)[b]	2.0 ± 0.14	0.8 ± 0.3
(S)-2-Methylbutyryl-CoA	18 ± 3 (*N* = 29)	4.1 ± 0.3	0.23 ± 0.06
n-Propionyl-CoA	24 ± 7 (*N* = 20)	0.83 ± 0.07	0.04 ± 0.01

[a] All values represent the standard deviation and 95% confidence intervals calculated as described in the text.
[b] *N*, number of determinations.

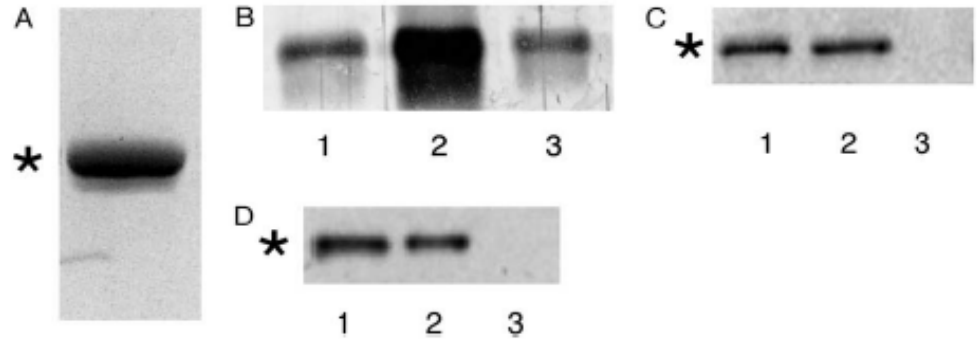

Figure 2: Western blot of wild type and Arg280Gln mutant iBD. **A**. Comassie A Blue staining of a 10% polyacrylamide SDS gel with 15 ng of purified wild type iBD. **B**. Western blot of crude *E. coli* cell extracts following expression of wild type (Lane 2) and Arg280Gln iBD (Lane 3). Samples were separated on a 10% polyacrylamide SDS gel. Equal amounts of 300 ng cellular protein were loaded on the gel. Lane 1 shows purified iBD. **C.** Western blot of crude cell extracts from COS-7 cells following expression of wild type (Lane 1) and Arg280Gln (Lane 2) iBD. Samples were separated on a 12% polyacrylamide SDS gel. Five micrograms of cellular protein were loaded in each lane. Lane 3 shows extract from cells trasfected with vector containing no insert. **D**. Western blot of crude extracts from normal (Lane 2) and patient (Lane 3) fibroblasts after separation on a 10% polyacrylamide SDS gel. 120 mg of cellular protein were loaded for each sample. Lane 1 shows purified iBD.

To characterize the effect of the Arg280Gln amino acid substitution identified in the patient on iBD activity, the mutation was introduced into the wild type prokaryotic expression vector, the cells were induced, and crude lysate was prepared as above. No activity could be detected in the extract with isobutyryl-CoA as substrate using a maximum amount of 127 μg of extract protein (up to 30 fold higher than used for assay of the extract from cells expressing the wild type vector). Western blot experiments with antiserum produced to the purified recombinant iBD confirmed that the mutant enzyme was expressed and was in the soluble cell supernatant from mutant cells, though at lower levels than for the wild type expression vector (Figure 2B).

The precursor forms of the mutant and wild type iBD were also expressed in COS-7 cells. Extracts from cells expressing the wild type iBD sequence had a specific activity of 3.6 ± 0.4 mU/mg cellular protein. No activity was detectable in extracts from cells transfected with the mutant vector, even when 2.5 fold more cellular protein compared to wild type extract was used in the assay (75 vs. 30 mg, respectively). Western blotting with iBD antiserum confirmed the presence of immunoreactive protein in extracts from

both transfected cell lines, though the level of mutant iBD was less than wild type (Figure 2C). Immunostaining and confocal laser scanning microscopy of transfected COS-7 cells revealed localization of both wild type and mutant iBD proteins to the mitochondria, the predicted location for the normal enzyme (Figure 3). Finally fibroblasts from the patient showed no immunoreactive iBD, while enzyme was present in control cells (Figure 2D).

Molecular modeling was used to generate a structural model of iBD as well as predict the effects of the patient mutation on iBD structure. Modeling of other ACADs has previously proven to be a robust method for this purpose due to the high level of conservation of the primary carbon backbone configuration in this gene family (20,22). The model generated for iBD, shown in Figure 4, reflects the conserved nature of the input structures, including the location of the predicted catalytic base (Glu376 in the mature protein). Arg302Gln (position 280 in the mature protein), mutated in the patient, is predicted to lie at the interface of interacting dimers within the mature homotetramer.

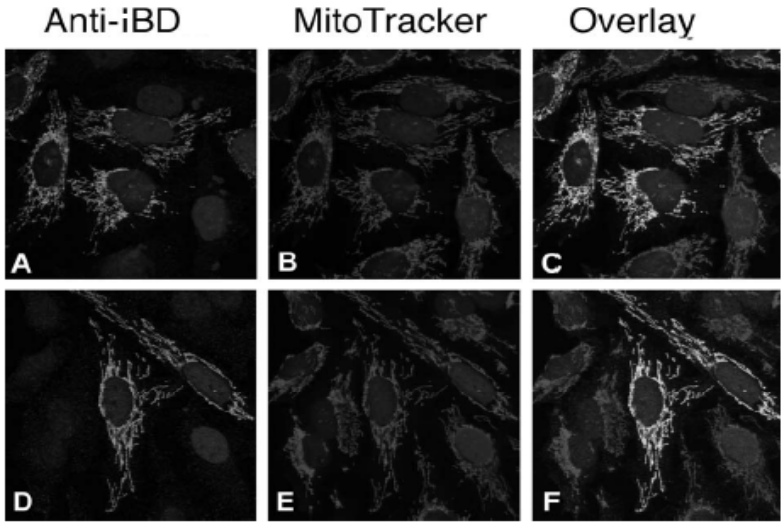

Figure 3. Localization of wild type and mutant iBD to mitochondria after expression in transfected COS-7 cells. Forty-eight hours after transfection with wild type iBD (**A**, **B**, **C**) and Arg280Gln (**D**, **E**, **F**) expression vectors, cells were incubated with the rhodamine (red) labeled MitoTracker (**B**, **E**) for 30 min at 37°C. Following fixation and permeabilization, cells were immunostained using anti-iBD polyclonal primary antibody, detected by an Alexa 488- conjugated (green) secondary antibody (**A**, **D**) and analyzed by CLSM. **C** and **F**. Overlay of the different optical sections shown in **A**, **B** and **D**, **E**, respectively. Nuclear DNA is counterstained with Hoechst 33258 (blue). Original magnification 1000x.

The relatively high specific activity of rat i2VD for both 2-methylbutyryl-CoA and isobutyryl-CoA compared to the human enzyme led us to hypothesize that iBD might be specific to humans, and thus represent a relatively recent gene duplication event. To examine this, Southern blotting of rat and genomic DNAs was performed using the human iBD and i2VD cDNAs as probes. Southern mapping studies confirmed the presence of a single copy each of the iBD and SBCAD genes (data not shown), indicating a more ancient evolutionary event. This is substantiated by the presence of a mouse sequence reported in the genetic databases with up to 90% homology to human iBD (Stratagene mouse macrophage Mus musculus cDNA clone #937306).

In order to examine this question further, we searched Genbank for sequences related to the ACADs (Table 2), and classified them on the basis of homology to each of the individual gene family members. Substrate specificity was then predicted on the basis of overall sequence homology, as well as conservation of key residues previously identified to be important in determining this feature.

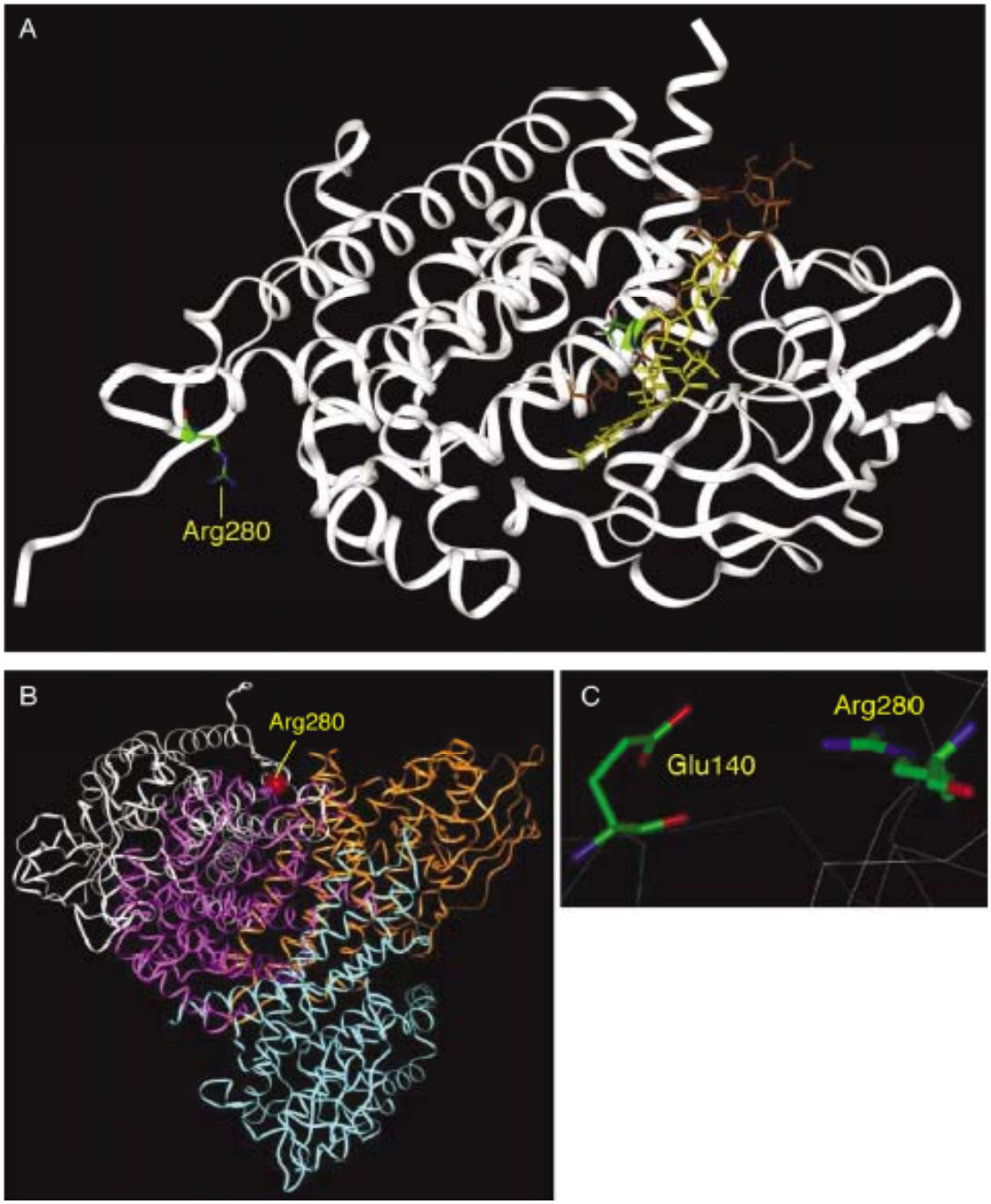

Figure 4. The predicted three dimensional structure of iBD and localization of the patient's mutation in the cleaved, mature protein. **A**. The structure of human iBD was predicted by molecular modeling as described in the text. **A** monomer of iBD with substrate and FAD is depicted. The location of Arg280 in the mature protein is indicated. The rendered atoms of Arg280 have been colored green for carbon, red for oxygen and blue for nitrogen. **B**. The position of Arg280 (rendered as a red sphere) in the predicted iBD tetramer structure is shown.Arg280 lies on the interface of interacting dimers within the mature homotetramer. **C**. Measurement of the molecular distance between the Arg280 from one iBD subunit and Glu140 from a neighboring subunit. Atom colors are as in **A**.

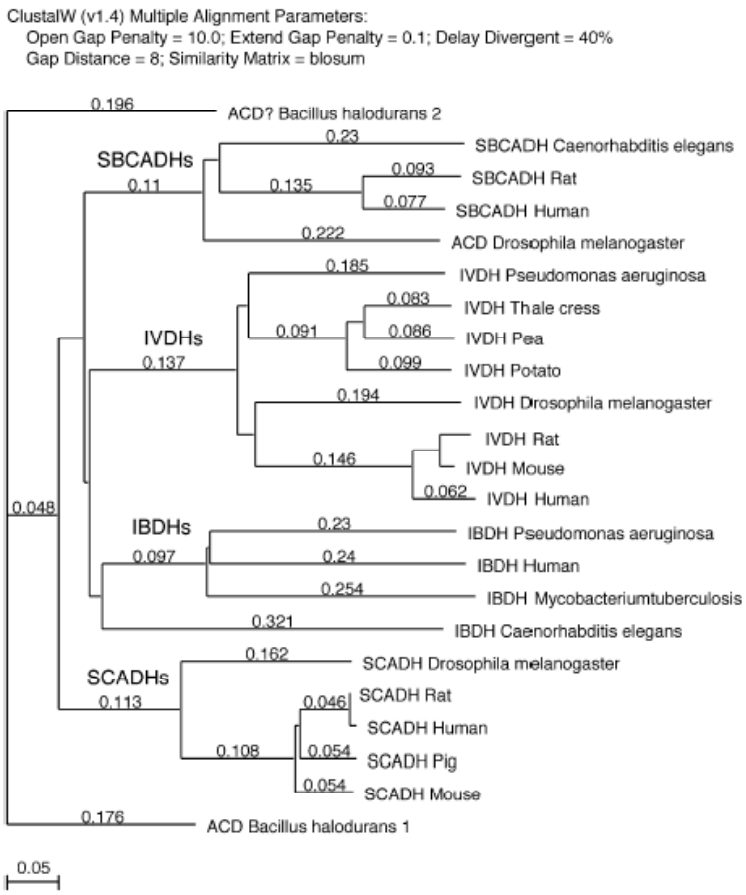

Figure 5. Phylogenetic tree of predicted iBD, i3VD, i2VD and SCAD amino acid sequences constructed using MacVector sequence analysis software version 7.0. Details regarding the species of origin and the database accession numbers of the various sequences are presented in Table 3 (see Abb. in Table 2).

A phylogenetic tree constructed from 23 ACADs from various species predicted to have branched chain activity is shown in Figure 5. Full length coding sequences likely to be i3VDs were found in at least 9 species, including 4 already shown by us to be i3VDs (human, rat, *C. elegans*, and pea). Sequences predicted to be iBDs and i2VDs were also clearly identified in a similarly wide range of species. These analyses identify human iBD as belonging to a distinct branch of the ACAD gene family with 20% amino acid identity and 32% similarity to other family members. It is more homologous to SCAD and i2VD than i3VD. Interestingly, bacterial proteins from *Mycobacterium tuberculosis* and *Pseudomonas aeruginosa* share the highest overall homology of the identified ACADs to iBD (64%), and thus might be potential candidates to be iBD homologues. Highly conserved key residues in the various ACADs are shown in Figure 6.

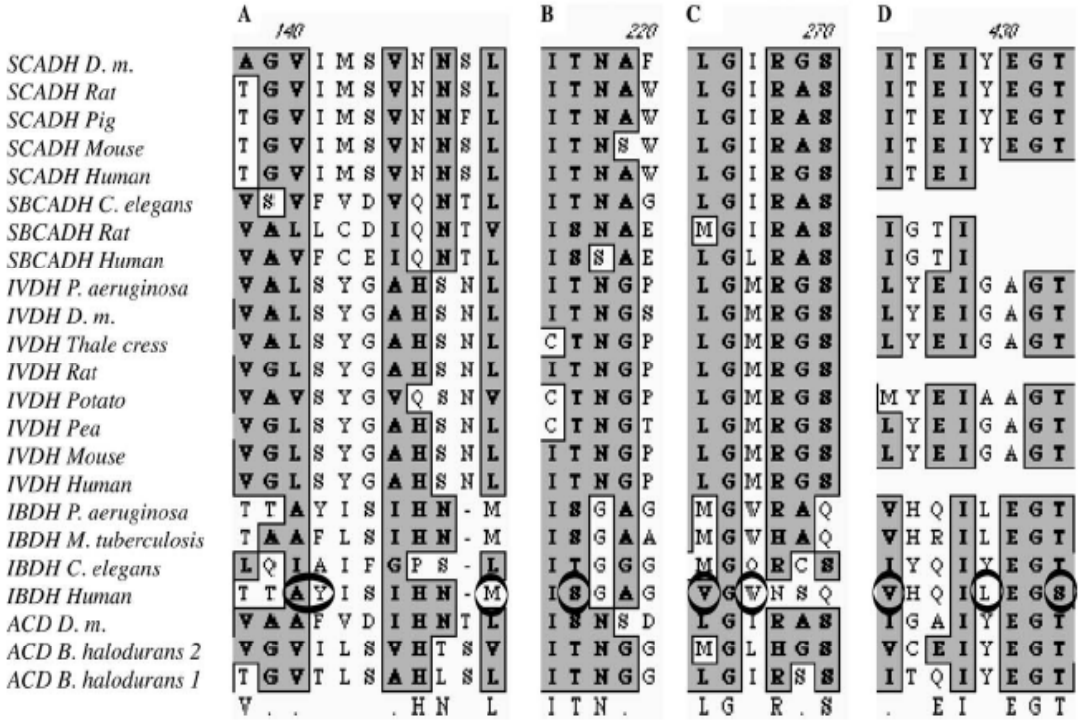

Figure 6. Alignment of key amino acid residues from predicted branched chain specific ACADs. Residues listed in Table 5 are circled. **A**. Ala99, Tyr100, and Met106; **B**. Ser171; **C**. Val215 and Trp217; **D**. Val371, Leu375, and Ser378 (see Abb. in Table 2).

Table 5
Amino acids predicted to be important among iBD, i3VD and i2VD

Amino acid residue			Predicted effect on substrate utilization
i3VD	iBD	i2VD	
Leu95	Ala99	Val104	Allows deeper pocket for substrate binding in iBD and i2VD
Ser96	Tyr100	Phe105	Similar structure in iBD and i2VD. Allows binding of other branched chain substrates
Leu103	Met106	Leu112	Allows accommodation of longer branched side chains in substrates in i2VD
Thr168	Ser171	Ser176	Blocks binding of other branched side chains in substrates in i3VD
Leu214	Val215	Leu220	Next to Leu95 in i3VD. Affects depth of substrate binding pocket
Met216	Trp217	Leu222	Affects depth of substrate binding pocket and accommodation of long chain substrates
Leu370	Val371	Ile376	Next to i3VD Leu95 in binding pocket. Determines depth of pocket
Gly374	Leu375	Tyr380	Blocks isovaleryl-CoA binding in iBD substrate binding pocket
Thr377	Ser378	Ala383	Alters trajectory of α–helix. Differentiates branched chain ACADs from others

2.5 Discussion

Dehydrogenation of 2-methylbutyryl-CoA and isobutyryl-CoA in the catabolism of isoleucine and valine was originally postulated to be mediated by a single enzyme, termed 2-methyl branched chain acyl-CoA dehydrogenase (3). The gene for this enzyme was subsequently termed *ACDSB* (denoting short-branched chain acyl-CoA dehydrogenase) to reflect the broad substrate specificity of the enzyme purified after expression in *E. coli* (6,7). More recently we have suggested that separate enzymes might exist to catalyze each reaction in the isoleucine and valine pathways (6,7,12-14), and preliminary studies of the substrate specificity of human *ACD8* overexpressed in COS-7 cells indicated that it had significant enzyme activity with isobutyryl-CoA (13). The current report confirms the existence of an isobutyryl-CoA dehydrogenase (IBD) specific to valine metabolism, unequivocally demonstrates identification of an ACAD with highest relative activity towards isobutyryl-CoA as substrate, and characterizes a mutation in the gene for this enzyme in a patient with cellular based evidence of a specific defect in valine metabolism (14). The identification of IBD completes the complement of ACADs for reactions known to be catalyzed by this family of enzymes. While it is, of course, possible that tissue specific forms of one or more of the ACADs may exist, as well as ACADs for reactions not previously associated with this family of enzymes, an extensive search of the available genetic databases including the human genome draft sequence has failed to identify any such candidate genes (J. Vockley, unpublished). In the context of cellular metabolism, it is likely that metabolism of isobutyryl-CoA and 2-methylbutyryl-CoA are mediated primarily by iBD and i2VD, respectively. There are lines of evidence in support of this. First, while both enzymes can utilize both substrates, their *K*m's towards their optimum substrate are much higher for the non-optimum than optimum substrates (7 and 50 fold higher, respectively for iBD and `i2VD` for their non-optimum substrates). Secondly, patients with iBD and `i2VD` deficiency show accumulation of only isobutyryl-CoA and 2-methylbutyryl-CoA derivatives, respectively, in blood and urine. The rather non-specific presentation of patients with both disorders makes consideration of each necessary in any child with unexplained developmental delay, failure to thrive, or apparent secondary carnitine deficiency. Furthermore, we have now identified additional individuals with deficiencies of both enzymes through expanded state newborn screening programs in North Carolina and Minnesota using tandem mass spectrometry (unpublished), all of whom were asymptomatic at diagnosis, and remain so on therapy. Long term follow-up of especially the patients diagnosed through newborn screening will be necessary to define the natural history of these diseases.

The Arg302Gln substitution identified in the iBD deficient patient leads to a loss of enzyme activity when the mutant enzyme is expressed in prokaryotic and eukaryotic systems. The mutant enzyme is appropriately targeted to mitochondria when expressed in COS-7 cells, but shows reduced stability in both expression systems and patient fibroblasts. Molecular modeling offers some insight into this phenomenon. The mutated amino acid residue at position 280 in the mature protein is conserved in i3VD and i2VD, homologous to Arg280 of i3VD and Arg286 of i2VD. In the iBD model, the distance from the catalytic site makes a direct effect of the patient mutation on substrate conversion unlikely. Rather, this residue lies in a position to interact with Glu140 of the opposite mature subunit (Figure 4), and likely plays a role in the interaction of the enzyme monomers/dimers, thus affecting their stability. Though the predicted distance between these residues in our model is greater than is optimal for such an interaction (4.6 A vs <3 A), it is important to note that the only positions of the amino acid residues within the individual subunits, and not their relative position to one another, have been optimized in the model. Thus it is possible that the two residues are actually in closer approximation than seen in our model. Consistent with this, it is has been suggested based on the crystal structure of porcine MCAD, that the homologous arginine in this mature enzyme (Arg281) is important for FAD binding and monomer dimerization, forming a hydrogen bond with the pyrophosphate moiety of FAD of the neighboring subunit of the MCAD dimer (24). Interestingly, mutation of the homologous residue has also been observed in patients with VLCAD (Arg326 in the mature protein) and i3VD (Arg282 in the mature protein) deficiency, underscoring the importance of this residue for correct ACAD function (20,27,28).

Examination of ACADs in the phylogenetic tree predicted to have branched chains specific from evolutionarily distant species provides an opportunity to evaluate the importance of various amino acid residues in determining substrate utilization in these enzymes. Selected portions of a multiple sequence alignment of 22 such ACADs are shown in Figure 6. Glycine residues at precursor positions 116, 186, 211, 243, 266, 297, 318, 406, 431 (75, 144, 165, 204, 215, 245, 264, 352, 355 in the mature iBD sequence) are highly conserved in all of the branched chain ACADs. The position of the presumed catalytic base of the enzymes is also highly conserved (numbered as residue in mature protein): Glu381 for human i2VD (11), Glu368 for human SCAD (17), and Glu254 for human i3VD) (18,23). The divergence of the position of the catalytic base in i3VD suggests that it is evolutionarily more distant from the other

family members. It has previously, been suggested that the gene for *IVD* evolved earlier than that for *ACADSB*, and that the gene for *ACADS* diverged recently relative to *ACADSB* (29,30). The more extensive sequence data now available confirms that *ACADS* belongs to an evolutionary branch of this gene family, which diverged earlier than the *ACADSB* and *IVD* genes. *ACADSB*, *IVD* and *IBD*, however, appear to be more closely related to each other than with *ACADS*. Overall, the divergence in the branched chain specific ACADs appears to be an evolutionarily ancient event as evidenced by the presence of apparent iBD sequences in *Mycobacterium tuberculosis* and *Pseudomonas aeruginosa*. Comparison of the known structure of human `i3VD` with our model of iBD, and one of human SBCAD that we have previously generated, allows prediction of a number of amino acid residues which are likely to be important in determining the ability to use branched chain substrates, along with optimum substrate specificity (22). These are listed in Table 5 and shown in Figure 6. *In vitro* mutagenesis experiments designed to alter these residues in a systematic fashion will allow a better understanding of the factors important in determining substrate specificity.

2.6 Conclusion

Our data confirmed further the exist of a new ACAD (ACAD-8 or iBD) that utilizes isobutyryl-CoA as its optimal substrate. Additionally, we have characterized a deficiency of this enzyme in a patient previously shown to have a defect in cellular metabolism of valine, indicating that iBD is specific to valine metabolism. Database searches reveal that the divergence of iBD from other ACADs active toward branched chain substrates is likely an evolutionarily ancient event. Further study of this group of enzymes will be useful in elucidating the molecular mechanisms for their utilization of branched chain substrates.

2.7 References

1- **Crane, F., and Beinert, H.** (1955) On the Mechanism of Dehydrogenation of Fatty Acyl Derivatives of Coenzyme A - Part II. The Electron-Transferring Flavoproteins. *J. Biol. Chem.* **218**:717-731.

2- **Ikeda, Y., Dabrowski, C., and Tanaka, K.** (1983) Separation and properties of five distinct acyl-CoA dehydrogenases from rat liver mitochondria. *J. Biol. Chem.* **258**:1066-1076.

3- **Ikeda, Y., and Tanaka, K.** (1983) Purification and characterization of 2-methyl-branched chain acyl coenzyme A dehydrogenase, an enzyme involved in isoleucine and valine metabolism, from rat liver mitochondria. *J. Biol. Chem.* **258**:9477-9487.

4- **Ikeda, Y., Okamura-Ikeda, K., and Tanaka, K.** (1985) Spectroscopic analysis of the interaction of rat liver short chain, medium chain and long chain acyl-CoA dehydrogenases with acyl-CoA substrates. *Biochemistry* **24**:7192-7199.

5- **Izai, K., Uchida, Y., Orii, T., Yamamoto, S., and Hashimoto, T.** (1992) Novel fatty acid boxidation enzymes in rat liver mitochondria. 1. Purification and properties of very-longchain acyl-coenzyme A dehydrogenase. *J. Biol. Chem.* **267**:1027-1033.

6- **Rozen, R., Vockley, J., Zhou, L., Milos, R., Willard, J., Fu, K., Vicanek, C., Low-Nang, L., Torban, E., and Fournier, B.** (1994) Isolation and expression of a cDNA encoding the precursor for a novel member (ACADSB) of the acyl-CoA dehydrogenase gene family. *Genomics* **24**:280-287.

7- **Willard, J., Vicanek, C., Battaile, K.P., Vanveldhoven, P.P., Fauq, A.H., Rozen, R., and Vockley, J.** (1996) Cloning of a cDNA for short/branched chain acyl-coenzyme A dehydrogenase from rat and characterization of its tissue expression and substrate specificity. *Arch. Biochem. Biophys*. **331**:127-133.

8- **Bennett, M., Rinaldo, P., and Strauss, A.** (2000) Inborn errors of mitochondrial fatty acid oxidation. *Crit. Rev. Clin. Lab. Sci*. **37**:1-44.

9- **Roe, C.R., and Ding, J**. Mitochondrial fatty acid oxidation disorders. In: Scriver, C., Beaudet, A.L., Sly, W., Valle, D., editors. The Metabolic and Molecular Basis of Inherited Disease. 8th ed. New York: McGraw-Hill; 2001. p 2297-2626.

10- **Wanders, R.J.A., Vreken, P., Den Boer, M.E.J., Wijburg, F.A., Van Gennip, A.H., and IJlst, L.** (1999) Disorders of mitochondrial fatty acyl-CoA b-oxidation. *J. Inher. Metab. Dis.* **22**:442-487.

11- **Binzak, B., Willard, J., and Vockley, J.** (1998) Identification of the catalytic residue of human short/branched chain acyl-CoA dehydrogenase by *in vitro* mutagenesis. *Biochim. Biophys. Acta.* **1382**:137-142.

12- **Gibson, K.M., Burlingame, T.G., Hogema, B., Jakobs, C., Schutgens, R.B.H., Millington, D., Roe, C.R., Roe, D.S., Sweetman, L., Steiner, R.D., Linck, L., Pohowalla, P., Sacks, M., Kiss, D., Rinaldo, P., and Vockley, J.** (2000) 2-Methylbutyryl-coenzyme A dehydrogenase deficiency: A new inborn error of L-isoleucine metabolism. *Pediatr. Res.* **47**:830-833.

13- **Andresen, B., Christensen, E., Corydon, T., Bross, P., Pilgaard, B., Wanders, R., Ruiter, J., Simonsen, H., Winter, V., Knudsen, I., Schroeder, L., Gregersen, N., and Skovby, F.** (2000) Isolated 2-methylbutyrylglycinuria caused short/branched-chain acyl-CoA dehydrogenase deficiency: Identification of a new enzyme defect, resolution of its molecular basis, and evidence for distinct acyl-CoA dehydrogenases in isoleucine and valine metabolism. *Am. J. Hum. Genet.* **67**:1095-1103.

14- **Roe, C.R., Cederbaum, S.D., Roe, D.S., Mardach, R., Galindo, A., and Sweetman, L.** (1998) Isolated isobutyryl-CoA dehydrogenase deficiency: An unrecognized defect in human valine metabolism. *Molec. Genet. Metabol*. **65**:264-271.

15- **Telford, E.A., Moynihan, L.M., Markham, A.F., and Lench, N.J.** (1999) Isolation and characterisation of a cDNA encoding the precursor for a novel member of the acyl-CoA dehydrogenase gene family. *Biochim. Biophys. Acta.* **1446**:371-6.

16- **Gustafson, S., Proper, J.A., Bowie, E.J., and Sommer, S.S.** (1987) Parameters affecting the yield of DNA from human blood. *Anal. Biochem*. **165**:294-299.

17- **Battaile, K., Mohsen, A.-W., and Vockley, J.** (1996) Functional role of the active site glutamate-368 in rat short chain acyl-CoA dehydrogenase. *Biochemistry* **35**:15356-15363.
18- **Mohsen, A.-W.A., and Vockley, J.** (1995) Identification of the active site catalytic residue in human isovaleryl-CoA dehydrogenase. *Biochemistry* **34**:10146-10152.

19- **Mohsen, A.A., and Vockley, J.** (1995) High-level expression of an altered cDNA encoding human isovaleryl-CoA dehydrogenase in *Escherichia coli*. *Gene* **160**:263-267.

20- **Mohsen, A.-W., Anderson, B., Volchenboum, S., Battaile, K., Tiffany, K., Roberts, D., Kim, J.-J., and Vockley, J.** (1998) Characterization of molecular defects in isovaleryl-CoA dehydrogenase in patients with isovaleric acidemia. *Biochemistry* **37**:10325-10335.

21- **Corydon, T.J.** (2000) Human and mouse mitochondrial orthologs of bacterial ClpX. *Mamm. Genome* **11**:899-905.

22- **Vockley, J., Mohsen, A.W., Binzak, B., Willard, J., and Fauq, A.** (2000) Mammalian branched-chain acyl-CoA dehydrogenases: molecular cloning and characterization of recombinant enzymes. *Methods Enzymol*. **324**:241-258.

23- **Tiffany, K.A., Roberts, D.L., Wang, M., Paschke, R., Mohsen, A.W.A., Vockley, J., and Kim, J.J.P.** (1997) Structure of human isovaleryl-coA dehydrogenase at 2.6 angstrom resolution - basis for substrate specificity. *Biochemistry* **36**:8455-8464.

24- **Kim, J.-J., and Wu, J.** (1988) Structure of the medium chain acyl-CoA dehydrogenase from pig liver mitochondria at 3-A resolution. *Proc. Natl. Acad. Sci. USA*. **84**:6677-6681.

25- **Kim, J.J.P., Wang, M., and Paschke, R.** (1993) Crystal structures of medium-chain acyl-CoA dehydrogenase from pig liver mitochondria with and without substrate. *Proc. Natl. Acad. Sci. USA*. **90**:7523-7527.

26- **Djordjevic, S., Pace, C.P., Stankovich, M.T., and Kim, J.J.P.** (1995) Three-dimensional structure of butyryl-CoA dehydrogenase from *Megasphaera esdenii*. *Biochemistry* **34**:2163-2171.
27- **Andresen, B.S., Bross, P., Vianeysaban, C., Divry, P., Zabot, M.T., Roe, C.R., Nada, M.A., Byskov, A., Kruse, T.A., Neve, S., Kristiansen, K., Knudsen, I., Corydon, M.J., and**

Gregersen, N. (1996) Cloning and characterization of human very-long-chain acyl- CoA dehydrogenase cDNA, chromosomal assignment of the gene and identification in four patients of nine different mutations within the VLCAD gene. *Hum. Mol. Genet.* **5**:461-472.

28- **Andresen, B.S., Vianeysaban, C., Bross, P., Divry, P., Roe, C.R., Nada, M.A., Knudsen, I., and Gregersen, N.** (1996) The mutational spectrum in very long-chain acyl-CoA dehydrogenase deficiency. *J. Inherit. Metab. Dis.* **19**:169-172.

29- **Nandy, A., Kuchler, B., and Ghisla, S.** (1996) Molecular evolution and substrate specificity of acyl-CoA dehydrogenases: chimaeric 'medium/long' chain specific enzyme from medium-chain acyl-CoA dehydrogenase. *Biochem. Soc. Trans*. **24**:105-110.

30- **Tanaka, K., and Indo, Y**. (1992) Evolution of the acyl-CoA dehydrogenase/oxidase superfamily. *Progress in Clinical and Biological Research - New Developments in Fatty Acid Oxidation*. **375**:95-110.

3 Chapter Ib

Human Isobutyryl-CoA Dehydrogenase: A New member of the Acyl-CoA Dehydrogenase family. Purification and Characterization.

3.1 Summary

Human isobutyryl-CoA dehydrogenase (iBD) is a novel member of the acyl- CoA dehydrogenases family. It is involved in valine metabolism and its defect causes the accumulation of isobutyryl-CoA and dilated cardiomyopathy. We have cloned cDNA encoding the mature form of the enzyme into an expression vector, pET21, and transformed it into *E. coli*. The recombinant human iBD was purified to homogeneity and characterized. iBD is a tetramer of four subunits of molecular weight of about 42.7 KDa. iBD has maximum activity with isobutyryl-CoA, 15% of its max activity with propionyl-CoA and very low activity with 2-methyl-butyryl-CoA. No activity was detected with n-butyryl-CoA or isovaleryl-CoA. Its measured pI was estimated to be 6.2. Results from experiments with thiol modifying reagents suggest that iBD thiol groups play a crucial role in enzyme structure and function.

3.2 Introduction

Acyl-CoA dehydrogenases (ACADs) form a family of, in the meantime, nine members that catalyze the α,β-desaturation of acyl-CoA conjugates, and transfer of electrons to the electron transfer flavoprotein (ETF). They are assumed to share the same chemical mechanism, however, they differ in their specificity for different types of fatty acids linked to CoA (1). This family can be differentiated into two subclasses. One comprises the five members VLCAD1, VLCAD2, LCAD, MCAD and SCAD that act on "straight chain" substrates, who, in turn, are degraded sequentially in the ß-oxidation cycle and are thus assumed to be passed down from the first to the last of the named enzymes (1). The second subclass encompasses the enzymes involved in degradation of fatty acid conjugates arising from amino acid catabolism. These are isovaleryl-CoA dehydrogenase (i3VD), 2-methylbutyryl-CoA or 2-isovaleryl-CoA dehydrogenase (i2VD), general acyl-CoA dehydrogenase (GAD), and the new member iBD to be

described in the present work. With the exception of VLCAD1 (VLCAD2 not characterized yet) that exists as a dimer, the ACADs are found in homotetrameric form with one molecule of flavin adenine dinucleotide (FAD) non-covalently bound to each monomer (2). A cDNA encoding the precursor for the new member of this family, ACAD-8, was originally isolated from human adult brain and skin fibroblasts (3). Based on sequence homologies it was proposed to code for a new enzyme of the ACAD family (3). Preliminary activity profiles obtained with heterologously expressed enzyme suggested that the protein was involved in the catabolism of branched chain amino acids (4,5). This was in line with the occurrence of specific genetic defects and their physiological consequences (5,6), and it was thus deduced that the enzyme was involved in valine catabolism and specifically in the dehydrogenation of isobutyryl-CoA. Accordingly the enzyme was named isobutyryl-CoA dehydrogenase (iBD) (6). Earlier studies had assigned this activity to "2-methyl-branched chain butyryl-CoA dehydrogenase" or i2VD (7). In this report we describe the purification and biochemical characteristics of this novel enzyme in comparison with those of the other members of the subfamily.

3.3 Materials and methods

3.3.1 Materials and reagents.

These were from the companies listed: Q-Sepharose FF, Superdex 200 and Superdex 200 prep grade HiLoad 26/60 (Amersham Pharmacia). Hydroxyapatite CHT10-I Ceramic (Bio-Rad). Hydroxyapatite (Fluka). Ferricenium hexafluorophosphate (Aldrich). Serva Blue R (Serva). Bacto™ Tryptone and Bacto® Yeast extract (Becton Dickinson BD). NZ Amine A (Interorgana). Ferritin, Aldolase and Catalase (Amersham Pharmacia). Lysozyme, Low-MW protein standard (Bio-Rad.). Cleland's reagent, Ellman´s reagent (Sigma), and all other, not specified chemicals from Sigma.

3.3.2 Instruments.

FPLC was from Pharmacia/LKB. HPLC was from Kontron.

3.3.3 Expression and purification of recombinant human iBD.

Different cells and expression systems were used for optimizing the expression of the iBD protein. The expression plasmid pET21-IBD was transformed into BL21 (DE3),

RosettaBlue^{TM} (DE3) and C41 (DE3) cells. Also, iBD was co-expressed with GroEL/ES in BL21 (DE3) cells. The overnight culture used to inoculate 500 ml of 2xYT containing antibiotic(s) then left to grow at least 8 hours. The 500 ml was used to inoculate 8 liters of 2xYT medium in 8-liter Fermentor (from B. Braun Biotech company, Germany) at 25^{o}C and left to grow to OD_{580} 0.8-1.0. iBD induced by using IPTG by final concentration of 0.5 mM. After 6 hours, the cells were harvested by centrifuging in 6 x 1-L bottles at 5,000 rpm (2600 x *g*) for 20 min Cell-pellets collected and flash frozen in liquid N_2 and stored at –20^{o}C for later use. The yield was usually 300-400 g cell pellets.

3.3.4 Protein extraction.

One hundred grams of cell paste were suspended in 50 ml of Buffer A (25 mM KPi, pH7.8; 5 μM DTT; 5% glycerol), lysozyme was added to a final conc. 10 μg/ml, the solution was incubated for 40 min and then sonicated for 3 x 5 min. The extract was centrifuged for 90 min at 18,000 rpm using and then again for 90 min at 55,000 rpm for clarification of the solution.

3.3.5 Purification.

For protein precipitation ammonium sulfate was added to the extracts to 35% saturation and the suspension centrifuged for 30 min. at 18,000 rpm. AS was then added to the supernatant to 70% saturation, followed by centrifugation for 30-60 min. at 18,000.rpm. The pellet was resuspended in buffer A and dialyzed against 2 x 4 L Buffer A, for 4 hours each at 4^{o}C, then loaded onto a Q-Sepharose column (3.5 x 15cm).

After loading, unbound protein was washed out with 700 ml of buffer A and then the iBD was eluted by application of a 50 mL gradient 0-35% of buffer B (buffer A + 1.0 M KCl). The yellow fractions were collected (≈120 mL, elution at 20-25% buffer B, Fractions 65-85). The supernatant was brought to 70% AS, the precipitate was centrifuged, the pellet was suspended in buffer A2 (5 mM KPi, pH 7.4; 10 μM DTT; 5% glycerol) and desalted by dialysis towards 1 x 4 L Buffer A2, 4 hrs at 4^{o}C. The resulting fraction was then concentrated to 2 mL and loaded onto a Hydroxyapatite column (Fluka, 25x2cm). Unbound protein was eluted with 100 ml buffer A2 and the

enzyme eluted upon replacing buffer A2 with buffer C (Buffer A2 + 25 μM FAD) and applying a 500 ml gradient to 20% of buffer B2 (1 M KPi, pH 7.4). Fractions containing activity were pooled, concentrated to ≈10 ml by Aminco Centeprep (cut-off 30 KDa.) and desalted by gel-filtration over Sephadex G15 using buffer A2. The enzyme solution was concentrated again and loaded on a ceramic CHI-10 Hydroxyapatite (BioRad, 10 x 2.5 cm). The enzyme was eluted with a volume gradient towards 10% of buffer B2, the enzyme eluting in the fractions at 4-6% Buffer B2. At this stage iBD is ≥95% pure. For further purification, and if needed, a gel filtration step on Superdex 200 prep grade HiLoad 26/60 in 25 mM KPi, pH 7.8 containing 150 mM KCl, 5% Glycerol, and 5 μM DTT was added (flow rate 1.0 ml/min).

3.3.6 Molecular weight determination.

The molecular mass of the iBD peptide chain was determined with MALDI-TOF (Bruker Biflex time-of- flight mass spectrometer, Bruker Daltonik, Bremen, Germany) equipped with a 26-sample SCOUT source, a nitrogen UV laser (λ_{max}=337 nm), and a delayed extraction system. A concentrated sample of iBD, 1 μl (≈7 mg/ml), was mixed with 1 μl matrix solution (super saturated α-cyano-4-hydroxycinnamic acid in acetonitrile: 0.1% trifluoroacetic acid in water, 2:1) on the MALDI-TOF target and allowed to dry at room temperature (8). iBD native molecular weight was estimated by gel filtration (Superdex 200, 25 mM KPi, pH 7.8, 150 mM KCl, 5% Glycerol, 5 μM DTT) and using standard proteins: Ferritin, Aldolase, Ovalbumin and carbonic anhydrase (MW of 440, 158, 45 and 29 KDa, respectively) as references.

3.3.7 Isoelectric focusing.

ProteoGel IPG strips (Sigma I-3156), with a pH range 5-8, 7 cm in length, and the IPGphor IEF system (Amersham Pharmacia) were used. A lyophilized sample, from 150-250 μl of 4 μM iBD was re-dissolved in rehydration buffer (2D-Manual, Amersham Pharmacia) and the same rehydration buffer containing the IBD was used for the rehydration of the strip for 15 hours. After IEF, the strip was equilibrated in the equilibration buffer containing DTT (2D-Manual, Amersham Pharmacia) for 1 hour and then applied to an SDS-PAGE gel. iBD was detected by chemiluminescence using

antibody specific for His-tagged iBD kindly provided by Dr. P. Bross (Aarhus, Denmark).

3.3.8 Spectroscopic methods.

Unless otherwise stated all spectrophotometric measurements were carried out at 25°C in 40 mM potassium phosphate buffer, pH 7.8, containing 5% glycerol. Acyl-CoA solutions were standardized spectrophotmetrically in 10 mM KP, pH 6.0 using ε_{260} =15.4 $mM^{-1}cm^{-1}$. Absorption coefficients for iBD were determined using the SDS method (9) and ε_{450} = 11.3 $mM^{-1}.cm^{-1}$ for free FAD (10).

3.3.9 Enzyme assays and pH-dependence of activities.

Activities were measured using the ferricenium assay (11). Measurements of pH-dependences were carried out in 40 mM buffer containing 5% glycerol and 150 mM KCl at the indicated pH values and at 25°C. iBD was ≈20 nM and the buffers used were: pH 5.0: acetate/KOH; pH 5.5: MES/KOH; pH 6.0-6.5: HEPES/KOH; pH 7.0-7.5; pH 8.0: Tris/HCL; pH 8.5-9.0: Tricine/KOH; pH 9.5-10.0: Glycine/KOH.

3.3.10 Anaerobic conditions.

Oxygen was removed from enzyme samples in Thunberg type cuvets by 5-6 cycles of flushing with oxygen–free argon / vacuum.

3.3.11 Reactivity of SH groups.

iBD, 1 μM, in 40 mM KPi, pH 7.8, containing 5% glycerol. Concentrations of DTNB: a) 4 μM, b) 1.3 mM DTNB). Both absorbance at λ_{412} and activities were measured at time intervals. The amount of reacted sulfhydryl groups was calculated using ε_{412} = 14150 $M^{-1}cm^{-1}$ (12,13,14). The activity was measured using the ferricenium assay.

3.4 Results

The cDNA encoding iBD gene was transfected into an *E. coli* expression vector (6), however, overexpression and purification of the iBD mature protein have not been straight-forward. Overexpression in BL21 (DE3) or C41 (DE3) systems resulted in low levels of protein expression as judged by SDS gel analysis. The protein yield using RosettaBlue^{TM}(DE3) was improved, but not that of activity. A substantial improvement was achieved when the bacterial chaperonin GroEL/ES was co-expressed with BL21 (DE3). Under these conditions about 300-400 g of cell-paste were obtained from an 8-liter fermentation that contained approximately 6-8 mg iBD protein based on activity estimates. The major problem encountered in first attempts to purify iBD (6) was its instability during the purification steps, this leading invariably to substantial or complete loss of activity. The reason for this was traced in an unexpectedly high reactivity of accessible SH groups. Enzyme stability was substantially increased by addition of 5 μM DTT to all buffers used. In particular this did improve dramatically the yields of the ammonium sulfate fractionation, and Q-Sepharose chromatography steps. The second factor affecting stability is the propensity of iBD to loose the cofactor FAD. To prevent this FAD was added to the buffers for the hydroxyapatite steps. Further, positive modifications were the use of Q-Sepharose instead of DEAE cellulose and of two, subsequent hydroxyapatite chromatography steps, the first using material from Fluka for a purification up to ≈70% followed by one using Ceramic hydroxyapatite from BioRad. The purity of the isolated iBD is >95 % as documented in Fig. 1. The presence of 5% glycerol enhances the stability of the enzyme for storing below –20˚C.

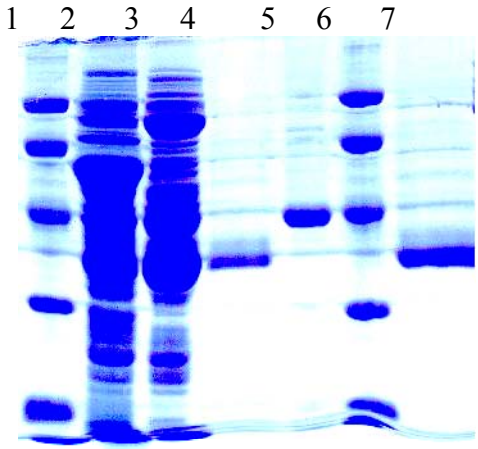

Fig. 1. SDS-PAGE of iBD at different stages of purification. Lanes 1 and 6; protein Standards; lane 2: cell extract after ammonium sulfate precipitation; lane 3: upon Q-Sepharose; lanes 4&7: ≈3 and ≈6 µg iBD after the second hydroxyapatite column; lane 5: pure human MCAD (MW = 44 KDa) as comparison.

The subunit molecular weight obtained by MALDI-TOF spectroscopy is 42.689 KDa ±100 Da. This compares to a MW = 42.692 KDa calculated from the amino acid composition derived from the cDNA sequence and indicating that the recombinant enzyme is not subject to secondary modifications upon expression in *E. coli.* The state of aggregation was estimated by gel filtration on Superdex 200 where iBD elutes as a symmetrical peak corresponding to a MW ≈170,000 KDa (not shown), and compatible with the presence of a tetramer. This is as with most ACAD enzymes with the exception of VLCAD that is a homodimer (2). The extinction coefficient of the flavin absorption band in the visible (see Fig. 2) was estimated as ≈ 14.1 $mM^{-1}cm^{-1}$ using the SDS method described in (9). This compares to 11.3 $mM^{-1}cm^{-1}$ for free FAD (10) and to values 12.3 to 14.8 for various ACADs; it is thus within the usual range for this family of flavoproteins.

The visible and ultraviolet absorbance spectrum of purified iBD is depicted in Fig. 2. Interestingly, pure iBD is obtained in a yellow form, although an associated green color can be noted during purification that is gradually lost. This contrasts with some other ACADs that are obtained in "green forms" due to tightly bound CoA-persulfide (15). This suggests that this CoA is bound comparatively less tightly to iBD. While the optical spectrum of iBD is typical for flavoproteins in having the two main bands

centered around 450 and 370 nm, it exhibits some subtle differences compared to those of e.g. MCAD, i3VD or i2VD that are taken to reflect minor changes at the active site, and can be used to differentiate the enzymes.

Table 1. Selected properties of human iBD and comparison with human SCAD, MCAD, i3VD and rat i2VD. All enzymes are tetramers.

Enzyme	iBD	SCAD[a]	MCAD[b]	i3VD[c]	i2VD[d]
Subunit MW	42	42	44	43	41.5
pI	6.2	4.6	4.8	5.1	5.5
λ_{max} (nm)	268:370: 444	269:356: 443	272:368: 446	269:370: 445	275:340: 435
λ_{max}≈270/≈450	5.4	9.3	6.1	5.4	10.3

a: Data taken from ref. 16, b: data taken from ref. 17&18, c: Data taken from ref. 19, d: Data taken from ref. 20.

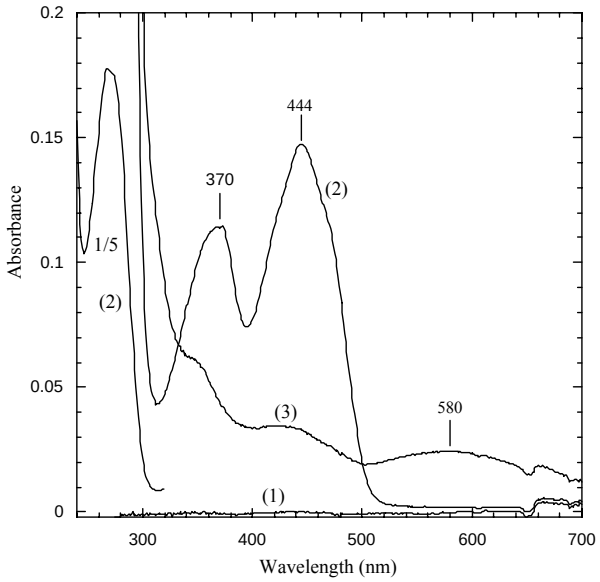

Figure 2. Spectral properties of iBD in the oxidized and reduced states. Curve (2) is for oxidized iBD, ≈10 μM in 40 mM KPi, pH 7.8, and containing 5% glycerol, upon anaerobisation. Curve (3) was recorded immediately upon addition of 80 μM isobutyryl-CoA (final concentration, spectrum corrected for dilution). The protein absorbance below 300 nm is reduced 5-fold for better comparison. (Curve 1 is the baseline).

The absorbance ratio of the maxima in the protein and visible region (268/444 nm in the present case) that is a characteristic for flavoproteins and reflects their degree of purity is ≈ 5.4 for iBD (Fig. 2). As a comparison the value for recombinant human MCAD is 5.7 (18).

Addition of the substrate isobutyryl-CoA under anaerobic conditions leads to formation of the reduced enzyme-2-methyl-acrylyl-CoA complex. This is characterized by the disappearance of the 450 nm band, and formation of a new species with maxima at 580 and 425 nm and a shoulder at ≈350 nm. The latter two belong to the reduced flavin chromophore, while the long wavelength band is due to the charge-transfer interaction between the reduced flavin as donor, and enoyl-CoA product as acceptor (21). This band is characteristic for most ACADs, it varies depending on the ACAD and the bound product in its position and intensity (21) and can be used to identify the species.
The isoelectric point of iBD was estimated as ≈ 6.2, a value that compares to 4.8 for MCAD (16) (Table 1).

As reported earlier, iBD shows highest activity with isobutyryl-CoA (6). We have extended the study of the activity profile to include activities measured with the ferricenium assay (11) and further substrates. Fig. 3 reports the behavior with the two best substrates isobutyryl-CoA and propionyl-CoA and the results are summarized in Table 2.

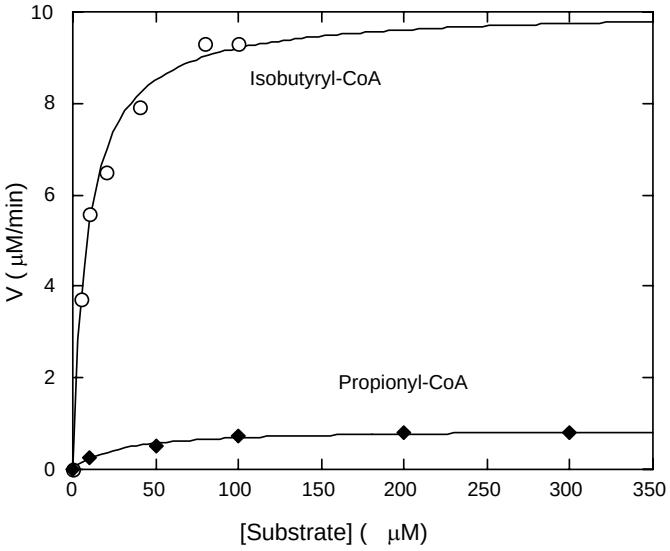

Figure 3. Dependence of the catalytic velocity of iBD from the substrate concentration Conditions: 40 mM KPi buffer, pH 7.8, 5% glycerol at 25°C and iBD = 20 nM for isobutyryl-CoA and 100 nM for propionyl-CoA.

Table 2**.** Catalytic parameters of iBD using the ferricenium and the ETF assays.

Substrate: R-CoA	Specific activity		Relative activity (%)		K_m	
	Fc K_{cat}/K_m ($\mu M^{-1}s^{-1}$)	ETF K_{cat}/K_m ($\mu M^{-1}s^{-1}$)	Fc	ETF	Fc µM	ETF µM
Isobutyryl-	0.02	0.8	100	100	9	2.6
Propionyl-	0.003	0.04	15	5	27	24
2-Methylbutyryl-	v.l.	0.23	n.d.	28	n.d.	18
n-Butyryl-	0	0	0	0	0	0
Isovaleryl-	0	0	0	0	0	0

v.l: very low activity; n.d.: not detected.

The ferricenium assay was carried out in 40 mM KPi buffer, pH 7.8, 5% glycerol at 25°C iBD = 20 nM for isobutyryl-CoA and 100 nM for propionyl-CoA. Data for the ETF assay taken in part from (6). With 2-methylbutyryl-CoA and using the ferricenium assay, iBD found to has very low activity in comparison to that with isobutyryl-CoA. However, using the ETF assay, the iBD activity was ≈28% in comparison to that with isobutyryl-CoA.

The effect of the pH on the activity of iBD with isobutyryl-CoA was studied using the ferricenium assay and the resulting profile is shown in Fig. 4.

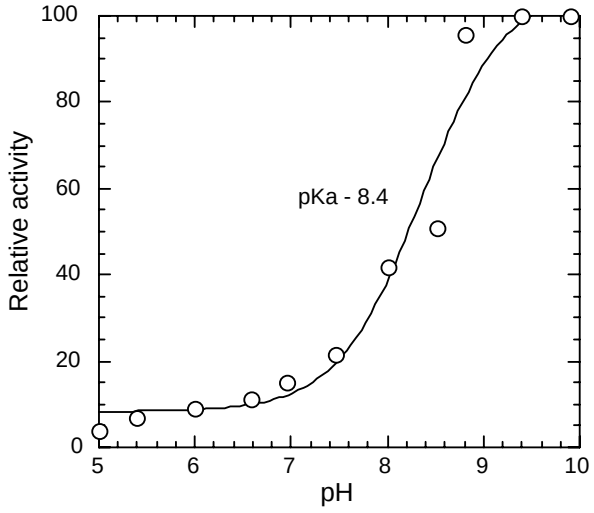

Figure 4. pH-dependence of iBD activity. Conditions as described in Experimental procedures.

There are several substrate analogs that have gained prominence as inhibitors or inactivators of ACADs (21). Some of these were found to be useful for mechanistic studies (22). Others, such as methylenecyclopropyl-acetyl-CoA are of natural origin. This analog (cf. Structure in Scheme 1) is a metabolite of hypoglycin, the causative agent of Jamaican vomiting sickness, and inactivates MCAD and SCAD via irreversible formation of covalent adducts (23, 24). It was thus of interest to verify whether iBD also would be a target for this family of inactivators. None of the analogs listed in Scheme 1 was found to inactivate iBD. This was particularly surprising in the case of cyclopropyl-formyl-CoA (see Scheme 1) since this molecule has the same skeleton as the best substrate, isobutyryl-CoA, and should have analogous steric requirements. The spectral perturbation observed upon addition of cyclopropyl-formyl-CoA to iBD (Fig. 5, insert) show that this analog does bind to the enzyme. However, over a period of 3 hrs under anaerobic conditions no further spectral changes ensue indicating that no dehydrogenation occurs (Fig. 5) and no activity was detected using the ferricenium assay of the treated iBD.

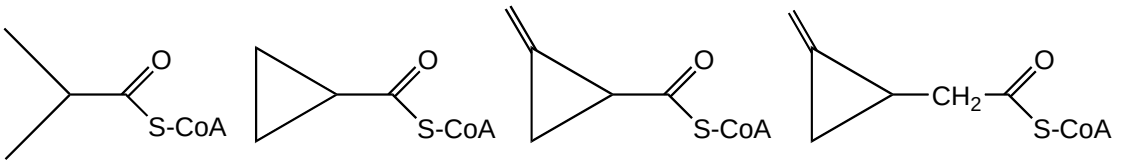

Isobutyryl-CoA CPF-CoA MCPF-CoA MCPA-CoA

Scheme 1. Structure of the substrate isobutyryl-CoA and of the analogs cyclopropyl-formyl-CoA (CPF-CoA), methylenecyclopropylformyl-CoA (MCPF-CoA) and methylenecyclopropylacetyl-CoA (MCPA-CoA).

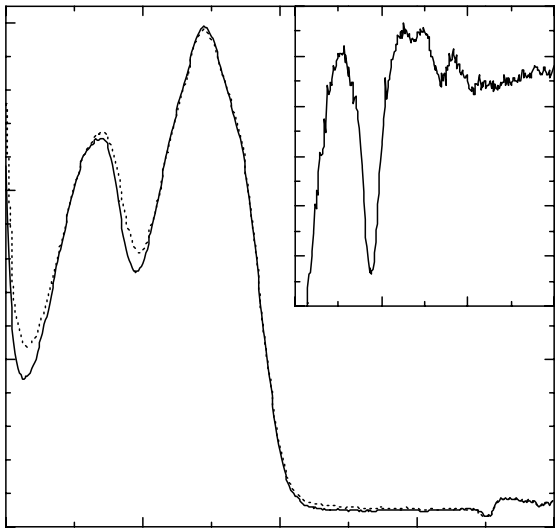

Figure 5. Interaction of iBD with CPF-CoA. Curve (—) is the spectrum of oxidized enzyme in 40 mM KPi buffer, pH 7.8, 5% glycerol at 25^{o}C under anaerobic conditions. Upon addition of 80 μM of CPF-CoA, the spectrum (---) that was obtained did not undergo modifications over a period of 3 hrs. The insert depicts the difference spectrum between free and complexed iBD.

Based on the observation that DTT substantially increases the stability of iBD, and on the fact that iBD contains 13 cysteines, we have carried out some experiments to assess the role of these groups in inactivation. The time dependence of the reaction of iBD with a 4-fold and 100-fold molar excess of DTNB, (Ellman´s reagent) is shown in Fig. 6 along with the course of the activity.

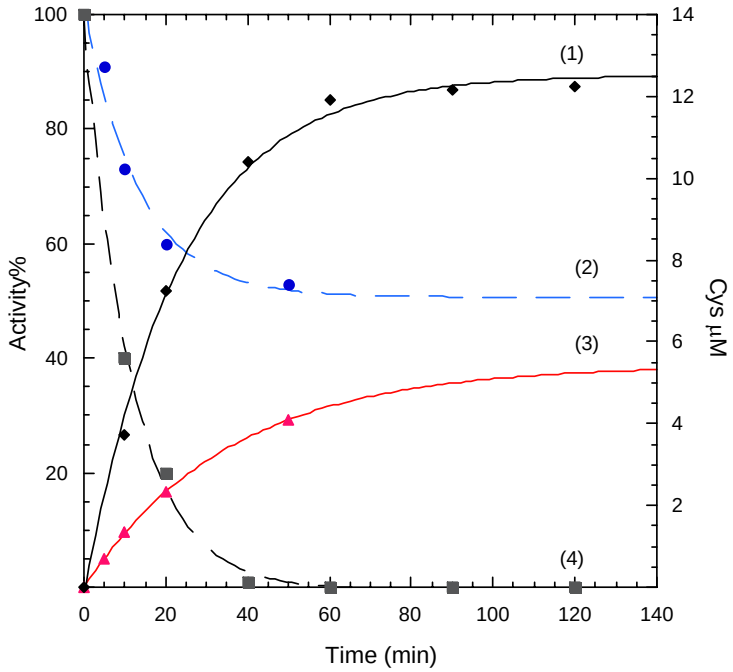

Figure 6. Time course of the reaction of iBD with DTNB. iBD, 1 µM, in 40 mM KPi, pH 7.8, containing 5% glycerol, was reacted with 1.3 mM and 4 µM DTNB. Curves (1) and (3) relate to the number of reacted –SH groups (observed OD at 412 nm /Ext coeff = 14150 $M^{-1}cm^{-1}$). Curves (2) and (4) represent the time course of the activity.

From the data in Fig. 6 it appears that all 13 cysteine residues present in iBD (extrapolated value for T_{∞} ≈12.7) react at similar rates, the processes shown in Fig. 6 being monophasic.

3.5 Discussion

Upon the discovery of MCAD and SCAD by Beinert's group in the mid 60' the other members of the ACAD family were discovered in rather rapid succession (25). Only recently iBD was identified in the human genome based on sequence similarities and was reported by Lench *et. al.* (3). The sequence similarity with the other members of the ACAD family are: 28% with GCD, 32% with VLCAD and LCAD, 33% with i3VD, 34% with MCAD, 36% with i2VD and 38% with SCAD (3). That this enzyme could be overlooked for such a long time probably has to do with his relative instability, and on the fact that i2VD has some activity in the dehydrogenation of isobutyryl-CoA, the product of catabolism of valine (20). The discovery of iBD was also promoted by the finding of a genetic defect in a 2-years old child with a reversible

cardiomyopathy and a deficiency in isobutyryl-CoA dehydrogenase activity in fibroblasts (6). iBD was found to be expressed in most tissues with low levels in liver and kidney (3).

iBD appears to have the closest relation to SCAD with which it shares the highest sequence similarity and which has the closed molecular mass (Table 1). It is slightly smaller than i3VD or MCAD and exists in solution as a homotetramer, a feature shared by most ACADs (18). A major difference between iBD and the other ACADs is in its relatively high isoelectric point (6.2) that compares to the more acidic values of i3VD, rat i2VD, MCAD and SCAD (Table 1). Analogies are also found in the pH dependence of the activity with its best substrate that reflects an apparent pK ≈8.4, similar to that of MCAD (pK ≈8.2) (17).

Different types of ACADs inhibitors were examined for iBD inhibition. Acetyl-CoA and acetoacetyl-CoA are known to inhibit ACADs enzymes (21). When examined with iBD, no inhibition found with either acetyl-CoA or acetoacetyl-CoA at 15 μM. In contrast, MCAD activity, for example, is inhibited by acetoacetyl-CoA (15). Another known inhibitor of ACADs is propionyl-CoA. It has been reported to inhibit partially, and very slow human SCAD (16) while inactivation of bovine SCAD is rapid and extensive (26). The finding of significant activity that is not accompanied by inhibition with propionyl-CoA suggests that this is an unique feature and that iBD might play a role in its degradation.

Some ACADs contain important cysteine residue(s) with iBD having the highest number, 13 that compares with 5 for SCAD, 7 for MCAD and 9 for I3VD. Sulfhydryl reagents are known to inhibit these latter enzymes (16, 27). iBD activity is completely inhibited by reagents that are known to affect the thiol groups in protein one example being DTNB (Fig. 6). As a further example, incubation with 5mM betaine (trimethylglycine) completely inhibits the activity of iBD, while it does not affect the activity of human wt-MCAD under similar conditions. These results suggest that cysteine residue(s) are important for the proper structure and/or activity of iBD and their reactivity might play a role in controlling iBD activity/degradation in vivo.

3.6 References

1- **Zhang, J., Zhang, W., Zou, D., Chen, G., Wan, T., Zhang, M., and Cao, X.** (2002) Cloning and functional characterization of ACAD-9, a novel member of human acyl-CoA dehydrogenase family. *Biochem. Biophys. Res. Commun*. **297**: 1033-42.

2- **Izai, K., Uchida, Y., Orii, T., Yamamoto, S., and Hashimoto, T.** (1992) Novel fatty acid β-oxidation enzymes in rat liver mitochondria.I: purification and properties of very long-chain acyl coenzyme A dehydrogenase. *J. Biol. Chem*. **267**:1027–33.

3- **Telford E.A., Moynihan L.M., Markham A.F., and Lench N.J.** (1999) Isolation and characterization of a cDNA encoding the precursor for a novel member of the Acyl-CoA dehydogenase gene family. *Biochim. Biophys. Acta*. **1446** , 371-376.

4- **Andresen, B., Christensen, E., Corydon, T., Bross, P., Pilgaard, B., Wanders, R., Ruiter, J., Simonsen, H., Winter, V., Knudsen, I., Schroeder, L., Gregersen, N., and Skovby, F.** (2000) Isolated 2-methylbutyrylglycinuria caused short/branched-chain acyl-CoA dehydrogenase deficiency: Identification of a new enzyme defect, resolution of its molecular basis, and evidence for distinct acyl-CoA dehydrogenases in isoleucine and valine metabolism. *Am. J. Hum. Genet.* **67**:1095-1103.

5- **Roe, C.R., Cederbaum, S.D., Roe, D. S., Mardach, R., Galindo, A. and Sweetman L.** (1998) Isolated isobutyryl-CoA dehydrogenase deficiency: An unrecognized defect in human valine metabolism. *Mol. Genet. Met*. **65**, 264-271.

6- **Nguyen, T. V., Andresen, B. S., Corydon, T. J., Ghisla, S., Abd El-Razik, N., Mohsen, A. A., Cederbaum, S. D., Roe, D. S., Roe, C. R., Lench, N. J., and Vockley, J.** (2002) Identification of isobutyryl-CoA dehydrogenase and its deficiency in humans. *Mol. Genet. Metab*. **77**: 68-79.

7- **Willard, J., Vicanek, C., Battaile, K.P., Vanveldhoven, P.P., Fauq, A.H., Rozen, R., and Vockley, J.** (1996) Cloning of a cDNA for short/branched chain

acyl-coenzyme A dehydrogenase from rat and characterization of its tissue expression and substrate specificity. *Arch. Biochem. Biophys*. **331**:127-33.

8- **Mann, M. and Talbo, G.** (1996) Developments in matrix-assisted laser desorption/inonization peptide mass spectroscopy. *Curr. Opin. Biotechnol*. **7**:11-19.

9- **Mayhew, S. G. and Massey, V.** (1969) Purification and characterization of lafvodoxin from *Peptostreptococcus elsenii*. *J. Biol. Chem.* **244**:794-802.

10- **Whitby, L.G.** (1953) A new method for preparing flavin-adenine dinucleotide. *Biochem. J*. **54**:437-42.

11- **Lehman, T. C., Hale, D. E., Bhala, A., and Thorpe, C.** (1990) An acyl-coenzyme A dehydrogenase assay utilizing the ferricenium ion. *Anal. Biochem.* **186**:280-4.

12- **Ellman, G. L.** (1959) Tissue sulfhydryl groups. *Arch. Biochem. Biophys*. **82**:70-7.

13- **Wright, K. S., and Viola, R. E.** (1998) Evaluation of methods for the quantitation of cysteines in proteins. *Anal. Biochem.* **265**:8-14.

14- **Riddles, P.W., Blakeley, R.L. and Zerner, B.** (1983) Reassessment of Ellman's reagent. *Methods Enzymol*. **91**, 49-60.

15- **Engel, P. C., and Massey, V.** (1971) Green butyryl-CoA dehydrogenase, an enzyme-acyl-coenzyme A complex. *Biochem. J.* 1**25**:889-74.

16- **Finocchiaro, G., Ito, M., and Tanaka, K.** (1987) Purification and characterization of short chain acyl-CoA, medium chain acyl-CoA and isovaleryl-CoA dehydrogenases from human liver. *J. Biol. Chem*. **262**:7982-7989.

17- **Bross, P., Jensen, T., Krautle, F., Winter, V., Andresen, B. S., Engst, S., Bolund, L., Kolvraa, S., Ghisla, S., Rasched, I. And Gregersen, N.** (1992)

Characterization of medium-chain acyl-CoA dehydrogenase (MCAD) with a point mutation associated with MCAD deficiency. *In* Prog. Clin. Biol. Res. : New developments in fatty acid oxidation (Coates, P. M. & Tanaka, K., Eds.). New York, Wiley&sons, **375**:473-478.

18- **Küchler, B., Abdel-Ghany, A. G., Bross, P., Nandy, A., Rasched, I., and Ghisla, S.** (1999) Biochemical characterization of a variant human medium-chain acyl-coA dehydrogenase with a disease-associated mutation localized in the active site. *Biochem. J*. **337**:225-30.

19- **Mohsen, A-. A. and Vockley, J.** (1995) High-level expression of an altered cDNA encoding human isovaleryl-CoA dehydrogenase in *E. coli*. *Gene* **160**:263-267.

20- **Ikeda, Y., and Tanaka, K.** (1983) Purification and characterization of 2-methyl-branched chain acyl coenzyme A dehydrogenase: an enzyme involved in isoleucine and valine metabolism from rat liver mitochondria. *J. Biol. Chem.* **258**:9477-87.

21- **Engel, P.C.** Acyl-CoA dehydrogenases, in *Chemistry and Biochemistry of Flavoproteins,* Mueller, F., Ed., CRC Press, Boca Raton, 2000, 597.

22- **Schmidt, J., Reinch, J., and McFarland, J. T.** (1981) Mechanistic studies on fatty acyl-CoA dehydrogenase. *J. Biol. Chem.* **256**:11667-70.

23- **Wenz, A., Thorpe, C., and Ghisla, S.** (1981) Inactivation of general acyl-CoA dehydrogenase from Pig Kidney by a metabolite of hypoglycin A. *J. Biol. Chem.* **256**:9809-12.

24- **Tanaka, K., and Ikeda, Y.** (1990) Hypoglycin and Jamaican vomiting sickness. *Prog. Clin. Bio. Res*. **321**:167-84.

25- **Beinert, H.** (1963) Enzymes, 2nd Ed. 7, 447-466.

26- **Okamura-Ikeda, K., Ikeda, Y., and Tanaka, K.** (1985) An essential cysteine residue located in the vicinity of the FAD-binding site in short-chain, medium-chain, and long-chain acyl-CoA dehydrogenases from rat liver mitochondria.
J. Biol. Chem. **260**:1338-45.

27- **Ikeda, Y., and Tanaka, K.** (1983) Purification and characterization of isovaleryl-Coenzyme A dehydrogenase from rat liver mitochondria. *J. Biol. Chem*. **258**:1077-85.

4 Chapter II

Acyl-CoA Dehydrogenases:

Study of the Effects of Genetic Defects on Enzyme Stability. Thermal Unfolding of Medium-Chain Acyl-CoA Dehydrogenase and Iso(3)valeryl-CoA Dehydrogenase.

4.1 Summary

Acyl-CoA dehydrogenases (ACAD) are key enzymes in the degradation of fatty acids and branched chain amino acids. Genetic defects affecting their function are increasingly recognized as being more widespread than originally thought. For the medium chain acyl-CoA dehydrogenase (MCAD), the K304E mutation is the most common genetic defect among Caucasian populations. In this study, ligand (substrate or substrate analogs) binding of recombinant wild-type MCAD and isovaleryl-CoA dehydrogenase (i3VD) and their genetic mutants K304E- and T168A-MCAD and A282V-i3VD is examined. The thermal stability of wild type and mutant proteins is also examined in the absence and presence of substrates or the corresponding 2-aza-acyl-CoA substrate analogs. Spectral studies show that binding of substrates and analogs to the mutant ACADs is generally weaker by approximately one order of magnitude compared to wild-type proteins. The thermal stability of MCAD (melting point ≈ 53.6 ºC) is significantly higher compared to i3VD (≈49.3 ºC). With the exception of the A282V-i3VD mutant that shows a marginal effect, a high degree of stabilization (5-11 ºC) is induced by substrate, i.e. by conversion into the reduced enzyme form complexed with product. Binding of 2-aza- substrate analogs increases the protein melting points by ≈0.5 ºC (A282V- and wt-i3VD) to 6 ºC.≈5.5 ºC. The results are discussed based on the 3D-structures of the enzymes and on the location of the mutations relative to domain interfaces, and substrate/cofactor binding pockets. It is concluded that in the case of K304E-MCAD thermal stability as such is not a major factor that might be related to the clinical phenotype. With the T168A-MCAD and A282V-i3VD mutants, however, the diminished thermal stability and minor stabilization by ligands must be regarded as an important factor contributing to the manifestation of the disease.

4.2 Introduction

Acyl-CoA dehydrogenases form a family of FAD-dependent enzymes that currently encompass nine members. They catalyze the same chemical step, the □,□-desaturation of acyl-CoA conjugates and differ in their specificity for different types of fatty acids linked to CoA (1). Two subfamilies can be differentiated. The first, comprising four members (vLCAD1, vLCAD2, MCAD SCAD), acts on "straight chain" substrates that are degraded sequentially in the ß-oxidation cycle (2). The second group also has four members (iBD, i2VD, i3VD, and GDH) that are active against branched chain substrates (3), while the only known substrate of GDH is glutaryl-CoA the degradation product of glutamic acid. The best-studied member of the first subfamily is medium chain acyl-CoA dehydrogenase (MCAD), an enzyme first discovered by Beinert (4). It has a comparatively broad spectrum of substrate utilization, is present at significant quantities in many organs (5), and the three dimensional structure has been elucidated (6). This enzyme gained medical relevance upon the discovery, some two decades ago, of an inherited genetic defect, which is among the most frequent ones in humans of northern European descent. A common point mutation causing a K304E replacement is found in 90% of mutant alleles from MCAD deficient patients, and has been associated with heterogeneous clinical symptoms and cellular defects (2). This amino acid is located in the long alpha helix H that forms part of the interface between subunits of the MCAD homotetramer and leads to impaired folding (7, 8), low expression of mature protein (8), instability (8), and a modified activity spectrum (8).

Another mutation in the MCAD gene in patients with MCAD deficiency leads to an amino acid replacement of threonine 168 to alanine. Threonine 168 is located in the active site of the enzyme in contact with the FAD cofactor and forms a hydrogen bond with the flavin N(5) (9). The mutant enzyme is stable but only partially active when expressed in heterologous systems. As is seen with the K304E mutation, patients with the T168A mutation present with heterogeneous symptoms (10).

i3VD is the best-studied member of the subfamily involved in the catabolism of amino acids (11); its biochemical properties have been addressed, and its 3D-structure is known (12). Several mutations leading to amino acid substitutions have been identified in patients with the clinical disorder isovaleric academia (IVA), caused by a deficiency

of i3VD. This disorder can cause a wide spectrum of clinical symptoms, and this may at least in part be related to the level of stability of the mutant enzyme (13). The most functional i3VD mutants reported are A282V, V342A, and R382L, each of which retains significant partial activity compared to wild type enzyme when produced in an *E. coli* system. (13).

In a general sense, many of the mutations discovered in patients with enzyme defects in mitochondrial ß-oxidation can be classified under the term "conformational diseases," with decreased folding of the mutant protein to a functional form under conditions of physiologic stress (14). This correlates well with the observation that clinical symptoms in these disorders are often exacerbated by otherwise unrelated underlying illness, especially when associated with fever. In this regard, MCAD and i3VD are appropriate candidates for studying in a semiquantitative manner, the extent to which mutations leading to amino acid substitutions affect protein folding and stability. Study of these processes will provide a better understanding of the effects of physiologic stress on mutant proteins in patients with these disorders, lead to the identification of amino acid motifs and physiologic conditions that help stabilize mutant proteins, and ultimately, the development of therapies designed to improve their stability. In this report, we present thermal stability studies of wild type, K304E-, and T168A-MCAD enzymes, and wild type and A282V-i3VD enzymes.

4.3 Materials and Methods

Desalting C18 cartridges (Sep-Pak Vac 35 cc C18 cartridges) were from Waters. Hexyl isocyanate (ACROS) and isopropyl isocyanate were from Aldrich. All other chemicals were from Sigma.

4.3.1 Preparation and purification of Acyl-CoA derivatives.

Octanoyl-CoA, isovaleryl-CoA, 2-azaisovaleryl-CoA 2-Azaoctanoyl-CoA were synthesized by published procedures (15). The crude products were desalted using C18 cartridges (30 ml, Waters, elution of salts with H2O, then of CoA's with 80% methanol). Purity of the products was analyzed by HPLC (Kroma system 2000) using 5 mM potassium phosphate buffer, pH 6.0, (pump A) and gradient from 5% to 35%

MeOH (pump B) over 20 minutes. The 2-Azaoctanoyl-CoA and 2-azaisovaleryl-CoA eluted at 16.2 minutes and 11.9 minutes, respectively. Purities were 94% and 92%, respectively. Concentrations were determined using ε_{260} = 20 $mM^{-1}cm^{-1}$ for saturated acyl-CoAs and ε_{258} = 16 $mM^{-1}cm^{-1}$ for 2-azaacyl-CoAs (16).

4.3.2 Purification of enzymes and mutants.

wt-MCAD (8), K304E- (8), T168A-MCAD (9), wt-i3VD (13, 17), A282V-i3VD (13) were heterologously expressed in *E. coli* and purified as described in the indicated literature.

4.3.3 Thermal Unfolding.

Thermal unfolding of MCAD, i3VD, and their mutants was monitored in 0.1 cm cuvettes using a Jasco J-500 spectropolarimeter at 222 nm. The cuvette was placed in a thermostatted cell holder. The temperature was raised continuously from 3°C to 93°C at a heating rate of 1.0°C/min. In all experiments, the enzyme concentration was ≈5 μM in 25 mM potassium phosphate, pH 7.5. Substrate stock solutions were prepared in the same buffer, and added at the indicated final concentration.

4.3.4 Data analysis.

The experimental data (θ_{222} = f(T)) were converted to plots of F_D = f(T) assuming that the ellipticities of the native and denatured state depend linearly on the temperature according to $\theta_N = \theta_{N,0} + a_N \times T$ and $\theta_D = \theta_{D,0} + a_D \times T$, respectively. $\theta_{N,i}$ and a_i are the coefficients of the linear function describing the pre-transitional and post-transitional portions of the unfolding trace. The fraction of the unfolded protein, F_D, at different temperatures is then given by:

$$F_D = (\theta - \theta_N) / (\theta_U - \theta_N)$$

The melting point, T_m, is the midpoint of transition where $\theta_N = \theta_U = 0.5$. The T_m was calculated from F_U-vs-T curve, where T_m is the temperature at F_D=0.5. The data were processed using the Origin® and KaleidaGraph programs.

4.4 Results and Discussion

4.4.1 Binding of ligands and substrates.

Acyl-CoA dehydrogenases, and in particular MCAD, for which the data are well documented (18), bind CoA conjugates very tightly, especially those that mimic structural and/or chemical properties of substrate or product (18). For example: Binding of enoyl-CoA to reduced MCAD has been estimated to be of the order of K_d = 90 nM (19). Several ACADs are isolated in green forms, where the color is attributed to tightly bound CoA-S-persulfide, which is carried along the purification procedure (20). As a basis for the understanding the effect of complex formation and change in redox state on thermal unfolding and stability we have studied some pertinent aspects involving binding/reaction of substrate and of some analogs.

It is important to note that the interaction of ligands/substrates with ACADs is a complex process (21) the salient components of which are shown in Scheme 1.

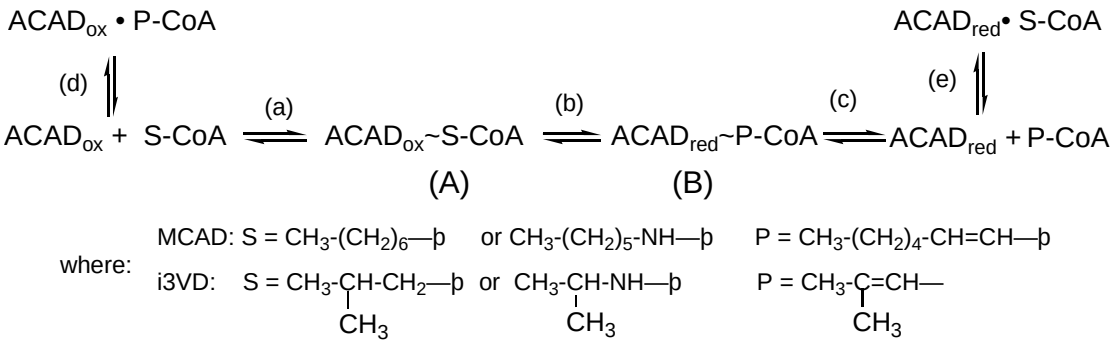

Scheme 1. Equilibria present in a system containing ACADs and substrates (adapted from (21, 22).

Step (a) is binding of ligand, and probably consists of several steps involving not shown intermediates that lead to complex (A). In the case of substrate step (b) follows, which reflects the chemical oxidoreduction equilibrium linking (A) to (B) (or $ACAD_{red}$~P-CoA), the complex of reduced enzyme with enoyl-CoA product. This probably consists of two species in rapid equilibrium (not shown) and is characterized by an intense green color arising from a charge transfer interaction (23). Product dissociation from (B) (step c) is thermodynamically very unfavorable (K_ds < 0.1 µM), relatively slow (24), and leads to free reduced enzyme $ACAD_{red}$. The latter, in turn, can bind excess substrate (step e), while free product (P-CoA) can bind to free oxidized

ACAD (step d). The reaction of substrate with ACAD will thus lead to a mixture of species that are linked by rapid or slow equilibria, and wherein the relative concentrations of the components will depend on temperature and on the concentrations of S-CoA and P-CoA. The second type of species is 2-aza-CoA substrate analogs that mimic substrate in forming complex (A). However, they cannot react to (B).

Only ligands that do not undergo chemical modification will form complexes in a straightforward manner (Scheme 1, step a). This is the case with 2-aza-substrate analogs that bind tightly to oxidized ACAD, but cannot reduce it (Scheme 1, step b) and can thus be used to study the binding step (a) selectively (16). 2-aza-octanoyl-CoA binds very tightly to oxidized, wild-type MCAD, the process being reflected by typical spectral perturbations with positive maxima reflected in the difference spectra in the 500 nm and negative in the 400-450 nm regions (16) (Table 1). We have complemented these data with binding studies of 2-aza-substrate analogs to the K304E-MCAD mutant, to i3VD and to the A282V-i3VD mutant. Binding of 2-aza-octanoyl-CoA to K304E-MCAD goes along with spectral effects (not shown) similar to those observed with wt-MCAD (16). However binding is less tight by approx. 1 order of magnitude (Table 1). The magnitude of this effect was unexpected since the mutation is not in the vicinity of the active center (8). A little more to follow, but need what follows first.

Binding of 2-aza-isovaleryl-CoA to wild-type i3VD is associated with changes in the UV-visible absorbance spectrum of the flavin chromophore of oxidized enzyme as shown in Fig. 1.Binding is relatively tight with a $K_d \approx 5$ µM, as derived from plots of the absorbance changes at various wavelengths (Fig. 1, insert A). While the pattern of the difference spectra (Fig. 1, insert B) is overall similar to that reported by Thorpe's group for MCAD (16), there is a substantial difference: With i3VD there is a weak, but significant absorbance extending from 500 to 800 nm observable both in the main panel and in the difference spectra which has a maximum around 510 nm (Fig. 1, panel B). This is due to a typical charge transfer transition and requires an acceptor, the oxidized flavin, and a ligand as a donor. However, 2-aza-iC5-CoA as such is not a donor. It becomes one upon deprotonation of the 2-aza-function:

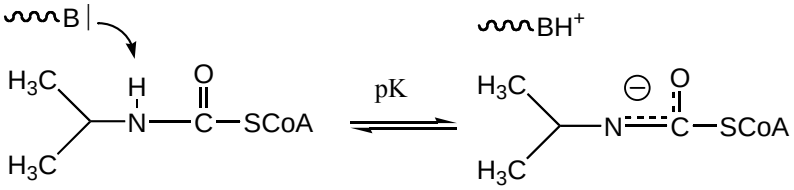

Scheme 2. Mode of deprotonation of the 2-aza-iC5-CoA analog at the active site of i3VD.

There are several examples of analogs that become deprotonated at the α-position upon binding to MCAD, two prominent ones being acetoacetyl-CoA and 3S-CoA (25, 26). The fact that the charge transfer intensity is weak could be due to a low intrinsic extinction coefficient. However it is more probable that under the specific conditions of Fig. 1, the equilibrium (pK) of Scheme 2 is not favoring deprotonation (see discussion in (26)). Determination of the pH dependence of this phenomenon is beyond the scope of the present work.

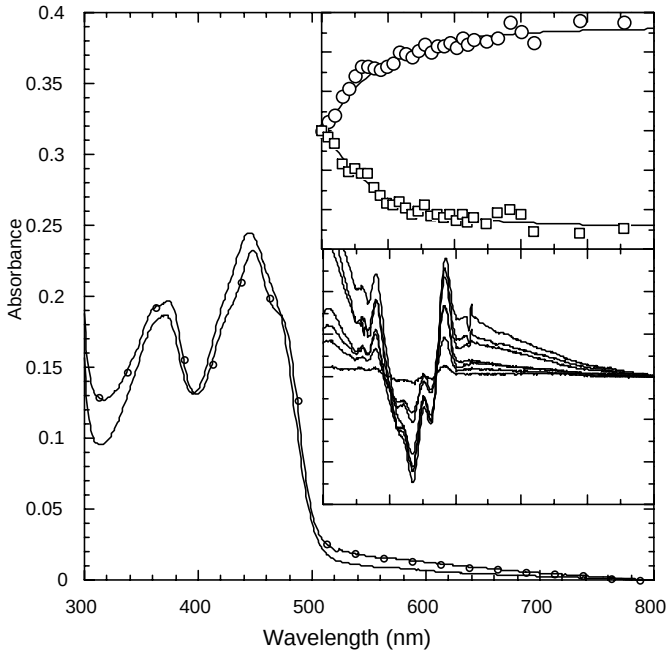

Figure 1. Binding of the substrate analog 2-aza-isovaleryl-CoA to wild-type i3VD. (Curve —) is the absorption spectrum of free enzyme, 18 μM in 50 mM Tris-Cl buffer, pH 8.0 and at 25^0C (Temp). Curve (—o—) was obtained upon addition of a total of 72 μM of the ligand (corrected for dilution). Insert (B) shows selected difference spectra obtained upon addition of (1): 2, 6, 16, 20, 46, 60 and (7) 96 μM of the ligand. Insert (A) depicts the changes at the indicated wavelengths as a function of added ligand. The lines are the fits obtained with the mass equation.

The A282V-i3VD mutant also binds 2-aza-isovaleryl-CoA as shown in Fig. 2. The perturbation of the oxidized flavin spectrum is comparable to that observed with wt-i3VD (compare difference spectra in Figs 1 and 2) suggesting that the binding modus is the same. However, the binding constant K_d is one order of magnitude higher, and this can be attributed to the larger volume of the valine isopropyl side chain compared to the methyl of alanine. This probably does not allow as tight a "closing" of the substrate binding cleft as shown in Fig. 9.

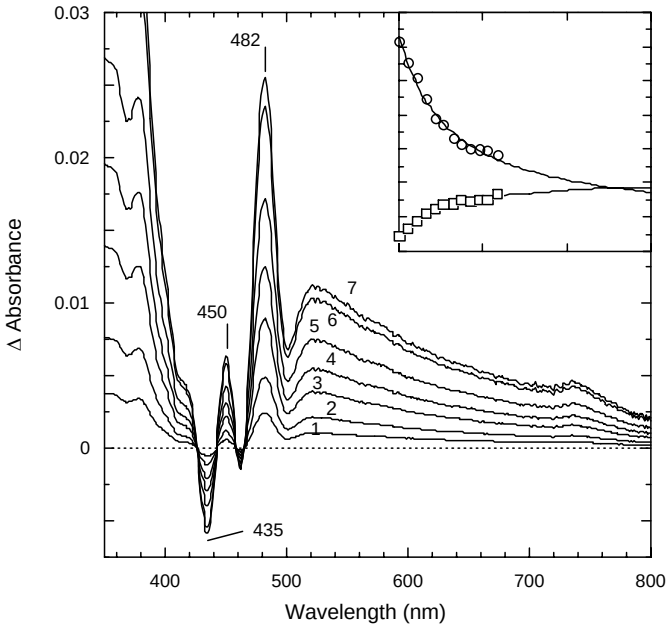

Figure 2. Interaction of A282V-i3VD with the substrate analogue 2-aza-isovaleryl-CoA. Conditions as detailed in the legend of Fig. 1, however at 25˚C. The increasing amounts of the ligand indicated in the insert were added to the enzyme, the starting spectrum of which corresponds to Curve (1) in Fig. 3. The main panel depicts the difference spectra obtained from subtraction of the initial spectrum from that at the given titration point. Only selected spectra are shown that correspond to addition of (1) = 8, (2) = 17, (3) = 25, (4) = 33, (5) = 98, (6) 192, and (7) = 312 µM ligand. All spectra and data points are corrected for dilution. Analysis of the primary data was done with the global fitting program "Specfit-32" (fit using data points at all wavelengths) and the traces in the main panel were obtained by a smoothing procedure of this program. The procedure yields an apparent K_d =36 ± 8 µM. The analysis in the insert is for the two wavelengths shown and yields apparent K_d's = 41 ± 9 (482 nm) and =42 ± 13 µM (580 nm).

Addition of substrate to ACADs leads to the set-up of the equilibria depicted in Scheme 1 (21,22). This represents a minimal scheme, the true situation being more complex (21) but not relevant for the present case. The apparent binding constant $K_{d,app}$ deduced from the dependence of spectral effects on the amount of added substrate will thus reflect all involved steps, and in particular step (b), the internal redox equilibrium of the system. In the case of wild-type MCAD $K_{d,app}$ for the best substrate octanoyl-CoA can be estimated as around 0.1-1 μM (24), and the prevalent species formed with a small excesses of octanoyl-CoA is reduced enzyme (23). $K_{d,app}$ is somewhat weaker for the K304E and T168A mutants (Table 1) as can be deduced from the extent of reduction of the oxidized enzymes under similar conditions (8, 9).

The behavior observed with i3VD is qualitatively similar. Addition of isovaleryl-CoA to i3VD leads to essentially complete reduction of the oxidized enzyme flavin with a $K_{d,app}$ ≤1 μM (Mohsen, Al-W., and Vockley, in preparation). This interaction is severely affected by the A282V mutation, where, in comparison to wt-i3VD, the $K_{d,app}$ of the mutant for the substrate is approx two orders of magnitude higher and reduction occurs only to approx 60 % (see decrease of the 450 nm absorbance in Fig. 3). This value is consistent with what has been observed with the measured K_m of the overall reaction using ETF reduction assay (13). It implies that the binding step (Scheme 1, a) is also impaired as with the 2-aza-analog, and that the internal redox equilibrium (Scheme 1, b) is not shifted completely to the right as with wt-i3VD.

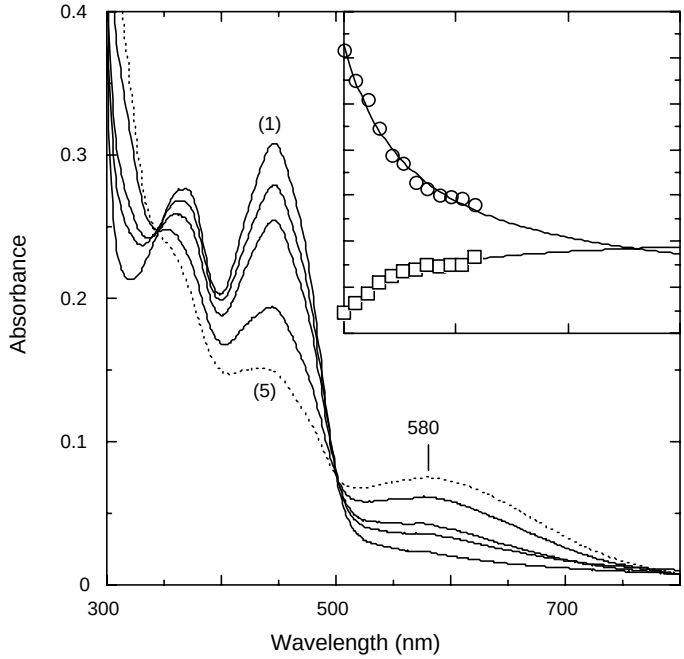

Figure 3. Interaction of A282V-i3VD with the substrate isovaleryl-CoA. The main panel depicts the anaerobic titration of the enzyme, ≈20 μM in 50 mM Tris-HCl, pH 8.0 and at 25ºC with increasing aliquots of isovaleryl-CoA. Curve (1), is the spectrum of free enzyme, (5) which was obtained in the presence of ≈60 μM substrate. The insert shows the dependence of the spectral changes at wavelengths where they are maximal from the indicated concentrations of added substrate. The full lines are the fits obtained using the mass law equation and yield "interaction constants" (apparent K_d's) of 30 ±6 μM (446 nm) and 26 ±6 μM (580 nm). The spectra and data points are corrected for dilution. See text for further details.

4.4.2 Thermal unfolding of wild-type MCAD and wild-type i3VD.

Thermal unfolding of wt-MCAD was measured as a function of temperature from 4 to 75°C as shown in Fig. 4. The data show that denaturation of wt-MCAD depends on its state of oxidation and on the presence of ligand. The melting range exhibited by unliganded, oxidized MCAD enzyme is broad, extending from ≈ 42˚C to ≈ 60˚C and involving a "shoulder" on the low-temperature side of the peak in addition to the main peak evident in the first derivative (Fig. 4, insert). This suggests the presence of different forms of the protein that vary in their thermal stability. This does not appear to be the case for i3VD (Fig. 5), since the first derivative profiles are comparatively sharp and symmetric. Comparison of the data for the two enzymes (Table 1) indicates that MCAD denatures at significantly higher temperature than i3VD.

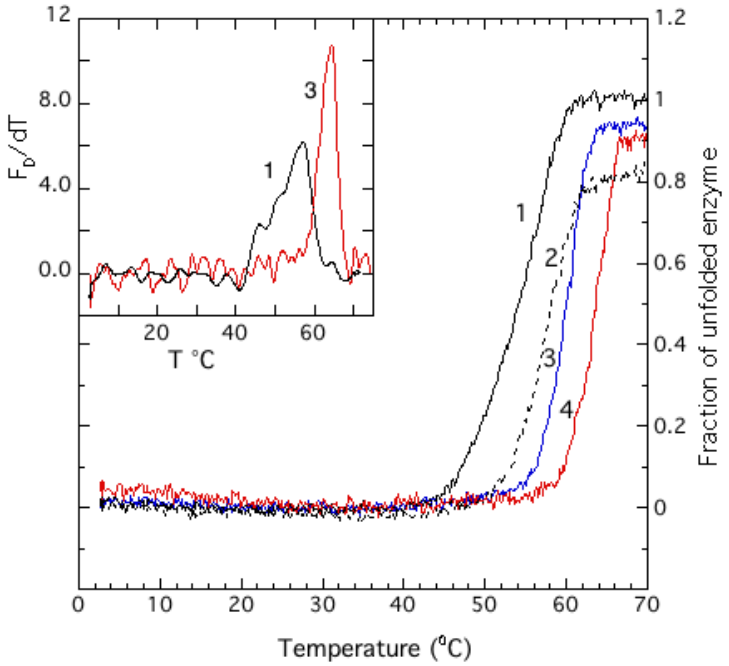

Figure 4. Thermal unfolding curves of wt-MCAD. Main panel: 1) in absence of substrate, 2) in presence of 20 μM 2-aza-C_8CoA, 3) and 4) in presence of 20 and 300 μM C_8CoA. The spectra were normalized for the values observed upon complete unfolding and changes were followed by far-UV CD at λ_{222} nm. Conditions are detailed in Materials and Methods. Insert: First derivative of the normalized CD spectra for curves 1) and 3).

As discussed above, substrate leads to reduction of ACADs and this is reflected by a stabilization corresponding to an increase of the melting point by 6 (i3VD) to 10 °C (MCAD) (Table 1, Fig. 5). In the presence of the substrate analog 2-aza-octanoyl-CoA that forms complex (A) (Scheme 1) there is an increases by ≈1-4 °C .The differences in melting temperatures induced by the two types of CoA (substrate vs substrate analog) thus reflect the differences in interaction with oxidized respectively reduced MCAD, and indicates that the factors involving the redox process are quantitatively more important than the binding process for thermal stability.

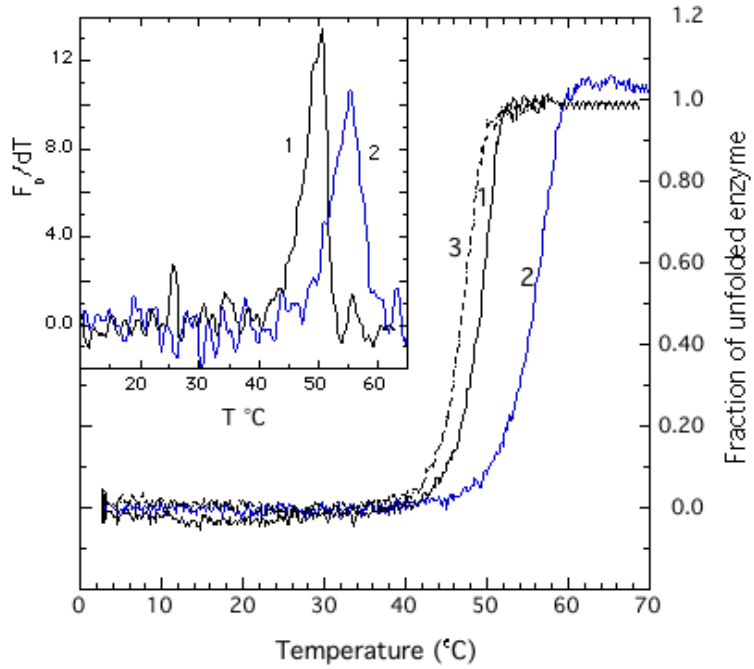

Figure 5. Thermal unfolding curves of wt-i3VD. Main panel: 1) in absence of substrate, 2) in presence of 20 μM iC_5CoA, and 3) in presence of 20 μM 2-aza-$i3C_5$CoA). The spectra were normalized for the values observed upon complete unfolding and changes were followed by far-UV CD at λ_{222} nm. Conditions are detailed in Materials and Methods. Insert: First derivative of the normalized CD spectra for curves 1) and 2).

Interestingly, with wt-MCAD the reaction with substrate and 2-aza-ligand leads to a much sharper transition (Fig. 2, insert) compared to unliganded enzyme. Thus free MCAD might exist in several conformers having marginally different melting temperatures and is converted upon ligand binding into single species corresponding to (A) or (B) respectively, Scheme 1. Comparison of the same phenomena for MCAD and i3VD uncovers greater stabilization by substrate for MCAD compared to i3VD (7-10 vs ≈6 °C, Table 1).

4.4.3 Effect of mutations on thermal stability.

In previous experiments the activity of the K304E and T168A mutants were compared to that of wt-MCAD by assessing the activity upon a definite time of incubation at different temperatures (8, 9). It was estimated that the activity decreases to 50% of the maximal value at ≈52 ºC for K304E mutant and at ≈41 ºC with T168A-MCAD. The latter was completely inactivated after 20 minutes incubation at 41 ºC (9). However, this type of experiments does not take into account the effect of ligands/substrate and

constitutes only a rather crude estimate. We have examined this directly with thermal denaturation experiments (Fig. 6). The K304E-MCAD mutant was found to unfold at ≈3.5 ºC lower than wt-enzyme. However, the K304E mutant protein responds to the presence/addition of the substrate octanoyl-CoA in a very similar way, the stabilizing effect is thus similar for both proteins (Table 1) consistent with an analogous thermodynamic effect accompanying formation of reduced enzyme. From this it can be concluded that thermal instability is not a major factor under physiological conditions that can rationalize the observed clinical effects. Previous studies had concluded that the mutation mainly affected the "conformation" of the enzyme (14) in addition to its capacity to be expressed in a soluble, active form (27), and to effects on its catalytic properties/specificity (8). The data presented here clearly support the importance of these factors. In contrast to the K304E mutant, the Thr168Ala-MCAD variant has a greatly reduced thermal stability both as the free protein, as well as in the presence of a substrate or substrate analog (Table 1) The extent of thermal destabilization of the T to A replacement suggests that it is a (major) source for protein instability *in vivo* and hence the molecular cause for the observed clinical symptoms.

4.4.4 Comparison of the data with structural information.

The present results provide a semiquantitative picture of the factors that affect unfolding of two of the best-studied members of the ACAD family, MCAD and i3VD. They also deepen and partially modify our understanding of the effects of genetically determined mutations affecting ACADs. Comparison of the melting temperatures for the various forms of MCAD and i3VD (Table 1, Figs 4-6) suggests that the thermal stability of wild type MCAD is rather high compared to that of i3VD; a difference of 6˚C in the melting temperature is significant. The overall supersecondary or quaternary structures of the two enzymes are very similar, with the exception of a disulfide bond between Cys318 and Cys323 in the loop connecting α-helices H and I present in i3VD (12). A specific reason for this difference is thus not evident. However, it can be speculated that factors such as FAD binding / affinity may also play a role in protein stability.

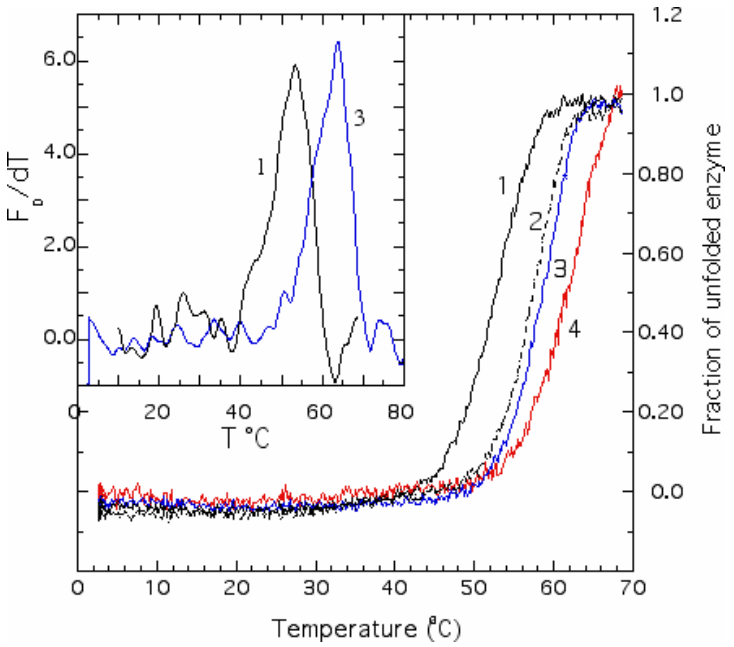

Figure 6. Thermal unfolding curves of K304E-MCAD. Main panel: 1) in absence of substrate, and 2) in presence of 20 µM 2-aza-C_8CoA, 3) and 4) in presence of 20 and 300 µM C_8CoA. The spectra were normalized for the values observed upon complete unfolding and changes were followed by far-UV CD at λ_{222} nm. Conditions are detailed in Materials and Methods. Insert: First derivative of the normalized CD spectra for curves 1) and 3).

While there are no quantitative data on the affinity of MCAD for FAD compared to i3VD, unpublished evidence suggests, by deduction, that FAD affinity is lower for i3VD. As an example T168 forms a tight H-bond to the flavin N-5 position (Fig. 7) and its removal as with the T168A mutant greatly reduces the affinity for FAD (9). Thus, while the T168A-MCAD mutant is produced in *E. coli*, and can be purified if FAD is present in buffers during purification, the corresponding T168A- i3VD mutant is substantially difficult to purify (Mohsen & Vockley, data not shown). This is consistent with a significantly weaker FAD binding with i3VD, and hence lowers stability for the wild-type, but specifically the A282V mutant. On the other hand, the thermal stability is substantially reduced compared to that of wt- and K304-MCAD (Table 1).

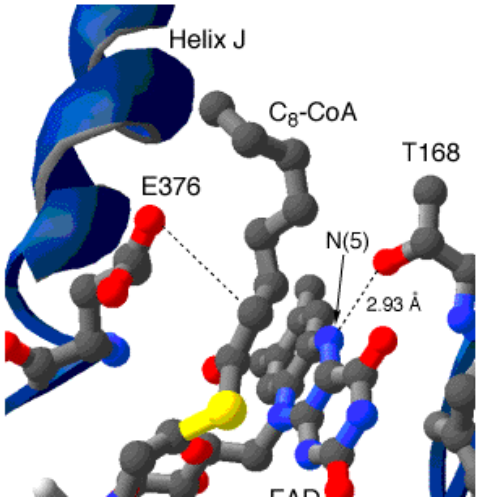

Figure 7. Active center of MCAD, and interaction of the flavin with Thr168. The T168-OH is placed approximately in the flavin plane and forms a tight H-bond to the N(5) of oxidized flavin. This interaction is juxtaposed to the substrate ß-C-H that delivers a hydride during the chemical event of catalysis. The E-376 carboxylate is positioned to abstract a H^+ from the substrate α-C-H.

Fig. 7 depicts the active center of MCAD and highlights the role of T168. The –OH group of this residue is positioned exactly in the projection of the flavin plane, and forms a tight H-bond (2.9 Å) with the flavin N(5), the entry point for hydride during catalysis. A specific role for such a H-bond also is probable since the activity of the mutant is substantially reduced (9): It is known (26) that for wt-MCAD the pK for the abstraction of a CoA ligand αC-H is lowered by ≥10 pK units at the active center. With T168A-MCAD the pK shift is much smaller (≤ 5 pK units, R. Gradinaru and S. Ghisla, unpublished) corresponding to a difference of ≈7 kcal/Mol. This is corroborated by the observation of a similar effect with wt-MCAD in which the native FAD cofactor has been replaced by its 5-deaza-FAD analog, which also cannot form such a H-bond (Gradinaru and S. Ghisla, unpublished). The Thr168-OH also affects the electronic properties of the flavin as manifested by the two fold decrease in stabilization of the neutral, blue flavin radical (9). In addition the Thr168-OH might serve in the fixation/positioning of the flavin (6, 9) and thus indirectly affect the stability of the protein since it is well established that binding of the FAD cofactor has strong effects on enzyme stability (28). In the context of enzyme stability it thus appears that this simple H-bond might be unusually strong as reflected by the large effect on enzyme

thermal unfolding. Along this line of reasoning it can be deduced that the substantially modified activity vs chain length profile exhibited by T168A-MCAD compared to wt enzyme (9) is due to enhanced flexibility at the active center.

The effect of genetic mutations on protein melting points is best represented by the K304E-MCAD case. Previous studies had concluded that the mutation mainly affected the "conformation" of the enzyme (14) in addition to its capacity to be expressed in a soluble, active form (27), and to effects on its catalytic properties and the chain length specificity (8). While the melting behavior confirms the diminished stability of this protein, the observed effect is comparatively small. Interestingly enough, substrate binding restores the thermal stability of the K304E mutant protein approx to the level of the wild-type enzyme. Inspection of the dimer-dimer interface domain of MCAD that is part of the homotetrameric native structure (Fig. 8) shows that K304 is part of a quaternary interaction of the groups R383, D300, K304 and D346 located on helices J, H and K (Fig. 8). Hence it is probable that a K304E mutation affects the strength of the salt bridge between D300 and R383 (Fig. 8) and that this, in turn, affects the tertiary/quaternary structure.

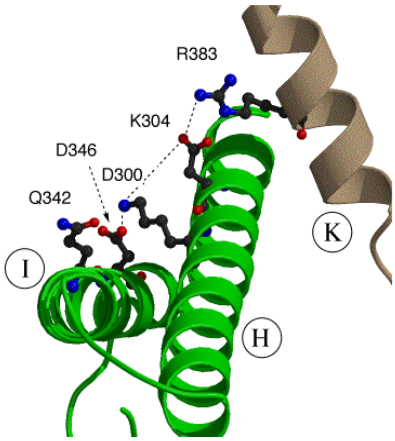

Figure 8. Three-dimensional representation of the location of the K304E-mutation in MCAD. Helices (I), (H) belong to different subunits than (K) of the interface domain of homotetrameric MCAD. It should be noted that the K304E-mutation is likely to affect the alignment of charges constituted by D346, K304, D300 and R383.

That this is reflected by an increase of apparent binding constants for ligand and substrate is surprising, but can be taken as a further example that modifications at one side of a protein envelope can have substantial effects at distant loci.

It was observed previously that expression of K304E-MCAD in COS-7 cells is severely diminished (29), that heterologous expression in *E. coli* is strongly dependent on the presence of coexpressed Gro-ESL proteins (27), and that purification could be achieved only when Gro-ESL is coexpressed (27). Once the protein had been purified it was stable enough to allow characterization of most of its enzymatic and biochemical parameters (8). In combination with the present data, it thus appears that the mentioned interactions of helices J, H and K are crucial for the recognition processes that lead to folding upon polypeptide synthesis and to import into mitochondria (27,7). This is in contrast with the case of T168A-MCAD. The latter protein can be expressed in *E. coli* in significant quantities, and can be handled without particular precautions provided the coenzyme FAD is present in excess at all stages (9).

Turning to i3VD, the lack of substantial changes in the melting temperature of the genetic A282V mutant in the presence of ligand and substrate, and as compared to wt-i3VD, is relevant. This is consistent with the mutant having substantially weaker affinities for ligands (Table 1) and also a ≈35 fold lower activity (13). Also in this case the A282V mutation is considerably distant from the active centers, of the same subunit (≈ 41 Å) or the neighboring subunit (≈ 17 Å). It is, however, in close proximity to residues constituting the FAD' adenine binding cleft (the prime sign denotes ligand or residue of the second subunit.) Fig. 9 shows that it is located at the monomer-monomer interface near the amino acid side chains of R280 and F290 that are in contact with the adenosyl moiety of FAD. In addition F283, which would be above the plain of the figure, is 3.5 Å away from the $C_{ß}$ of the A282 and 3.2 Å away from the FAD' adenine, apparently providing π-π interaction to the latter.

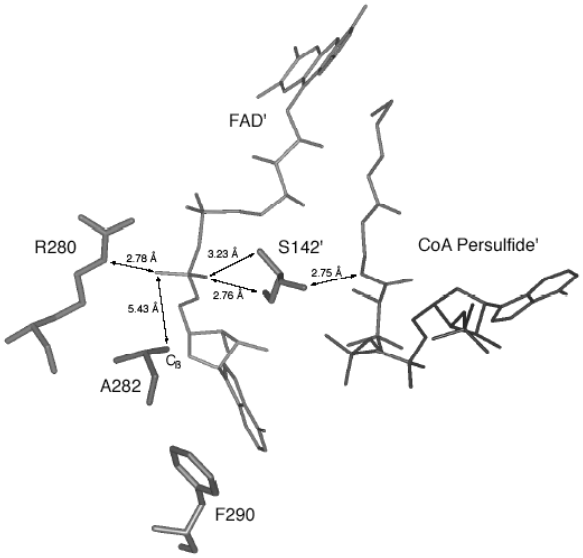

Figure 9. Position of A282 in i3VD relative to the cofactor FAD. This group is located near the interface of two subunits of the homotetrameric enzyme and in close proximity to the adenylate moiety of FAD. In the A282V mutant the larger size of the valine side chain is likely to "force open" the cleft serving for the binding of the FAD AMP moiety. Adapted from (Tiffany et al., 1997) (12).

Examination of the arrangements in Fig. 9 suggests that replacement of alanine with a valine would affect binding of FAD by disrupting the interactions of its AMP moiety with the above residues. This, in turn, might affect the interactions of S142' with the adenosyl moiety of FAD and the pantetheine moiety of the CoA ligand and consequently impair binding of the latter. Another possible effect for the A282V replacement is that the valine side chain in the mutant would force the side chain of F283, which is 4 Å away from the phosphate of the AMP' moiety of the i3V-CoA' in the published model (12), to adopt a slightly different conformation bringing it closer to this possibly charged phosphate and hence disrupting substrate binding.

It has been difficult to show genotype/phenotype correlations for mutations identified in patients with MCAD deficiency. Heterogeneous symptoms have been reported in patients with the common K304E mutation as well as in others seen in more than one patient. The present data substantiate the assumption that with this mutant thermal instability as such is not a major factor in disease manifestation. With the T168A mutation, however, thermal instability is much more pronounced arguing that it is a major molecular cause for the observed symptoms.

Table 1. Apparent melting points of MCAD, i3VD and of mutants and effect of substrate or ligand binding.

	Enzyme, Form	Substrate / Ligand Structure	Concentration µM	$\Delta\Delta T_m$ ±0.5 °C	Substrate/Ligand (apparent) K_d
MCAD	Wild-type, ox	None		56.4	-
	ox/red	C_8-CoA,	20	63.5	0.1-1 µM (15)
	red	C_8-CoA,	300	66.9	
	ox	2-aza-C_8-CoA	20	59.3	0.05 µM (15)
	K304E, ox	None		53	-
	ox/red	C_8-CoA	20	60	≥ 1 µM (a)
	red	C_8-CoA	300	64	
	ox	2-aza-C_8-CoA	20	59.1	≈0.5 µM
	T168A, ox	None		46.7	-
	ox/red	C_8-CoA	20	52.5	≥ 1 µM (a)
	red	C_8-CoA	300	58.1	
	ox	2-aza-C_8-CoA	20	52.1	nd
i3VD					
	Wild-type, ox	None		50.5	-
	ox/red	iV-CoA	20	55.4	≤1 µM (b)
	ox	2-aza-iV-CoA	20	50.9	≈5 µM
	A282V, ox	None		48.2	-
	ox/red	iV-CoA	20	48.5	≈30 µM
	ox	2-aza-iV-CoA	20	48.6	≈40 µM

The abbreviations ox, red and ox/red stand for oxidized, reduced, or a mixture of these species. (a) As explained in the text this value is a rough estimate that reflects the equilibrium situation described by Scheme 1. (b) Mohsen, W., and Vockley, J., unpublished.

Patients having i3VD mutations that lead to an enzyme that has partially reduced activity and/or stability, tend to have milder clinical symptoms than those with mutations leading to lack of enzyme protein at the cellular level. In such cases, reduced thermal stability of a mutant enzyme may play a role in the development of symptoms only during times of illness, especially those associated with fevers. Study of additional patients and mutations will be necessary to substantiate this.

4.5 References

1- **Zhang, J., Zhang, W., Zou, D., Chen, G., Wan, T., Zhang, M., and Cao, X.** (2002) Cloning and functional characterization of ACAD-9, a novel member of human acyl-CoA dehydrogenase family. *Biochem. Biophys. Res. Commun*. **297**: 1033-42.

2- **Gregersen, N., Andresen, B. S., Corydon, M. J., Corydon, T. J., Olsen, R. K., Bolund, L., and Bross, P.** (2001) Mutation anaylsis in mitochondrial fatty acid oxidation defects:Exemplified by acyl-coA dehydrogense deficiency with special focus on Geneotype-Phenotype relationship. *Hum. Mut.* **18**:169-89.

3- **Nguyen. T. V., Andresen, B. S., Corydon, T. J., Ghisla, S., Abd El-Razik, N., Mohsen, A. A., Cederbaum, S. D., Roe, D. S., Roe, C. R., Lench, N. J., and Vockley, J.** (2002) Identification of isobutyryl-CoA dehydrogenase and its deficiency in humans. *Mol. Genet. Metab.* **77**: 68-79.

4- **Beinert, H**. (1963) *Enzymes*, 2nd Ed. **7**, 447-466.

5- **Nagao, M., Parimoo, B., and Tanaka, K.** (1993) Developmental, Nutritional, and Hormonal Regulation of Tissue-specific Expression of the Genes Encoding Various Acyl-CoA Dehydrogenases and a-Subunit of Electron Transfer Flavoprotein in Rat. *J. Biol. Chem.* **268**:24114-24.

6- **Kim, J. J. P., Wang, M., and Paschke, R.** (1993) Crystal Structures of Medium-Chain Acyl-CoA Dehydrogenase from Pig Liver Mitochondria with and Without Substrate. *Proc. Natl. Acad. Sci. USA*. **90**: 7523-7.

7- **Saijo, T., Welch, W. J., and Tanaka, K.** (1994) Intramitochondrial folding and assembly of medium-chain acyl-CoA dehydrogense (MCAD)-demonstration of impaired transfer of K304E-variant MCAD from its complex with Hsp60 to the native tetramer. *J Biol Chem.* **269**:4401-8.

8- **Kieweg, V., Kräutle, F. G., Nandy, A., Engst, S., Vock, P., Abdel-Ghany, A. G., Bross, P., Gregersen, N., Rasched, I., Strauss, A., and Ghisla, S.** (1997) Biochemical characterization of purified, human recombinant Lys304→Glu medium-chain acyl-CoA dehydrogenase containing the common disease-causing mutation and comprison with normal enzyme. *Eur. J. Biochem.* **246**:548-56.

9- **Küchler, B., Abdel-Ghany, A. G., Bross, P., Nandy, A., Rasched, I., and Ghisla, S.** (1999) Biochemical characterization of a variant human medium-chain acyl-coA dehydrogenase with a disease-associated mutation localized in the active site. *Biochem. J.* **337**:225-30.

10- **Andresen, B.S., Bross, P., Udvari, S., Kirk, J., Gray, G., Kmoch, S., Chamoles, N., Knudsen, I., Winter, V., Wilcken, B., Yokota, I., Hart, K., Packman, S., Harpey, J.P., Saudubray, J.M., Hale, D.E., Bolund, L., Kolvraa, S. and Gregersen, N.** (1997) The molecular basis of medium-chain acyl-CoA dehydrogenase (MCAD) deficiency in compound heterozygous patients: is there correlation between genotype and phenotype?. *Hum. Mol. Genet.* **6**: 695-707.

11- **Tanaka, K., Ikeda, Y., Matsubara, Y., and Hyman, D.** (1987) Molecular basis of isovaleric academia and medium chain acyl-CoA dehydrogense deficiency. *Enzyme* **38**: 91-107.

12- **Tiffany, K. A., Roberts, D. L., Wang, M., Paschke, R., Mohsen, A. A., Vockley, J., Kim, J. J. P.** (1997) Structure of human isovaleryl-CoA dehydrogenase at 2.6 A resolution: structural basis for substrate specificity. *Biochemistry* **36**:8455-64.

13- **Mohsen, A. A., Andreson, B. D., Volchenboum, S. L., Battaile, K. P., Tiffany, K., Roberts, D., Kim, J., and Vockley, J.** (1998) Characterization of molecular defects in Isovaleryl-CoA dehydrogense in patients with isovaleric academia. *Biochemistry* **37**:10325-35.

14- **Bross, P, Corydon, T. J., Andresen, B. S., Jorgensen, M. M., Bolund, L., and Gregersen, N.** (1999) Protein misfolding and degradation in genetic diseases. *Hum. Mut.* **14**:186-98.

15- **Seubert, W.** (1960) S-Palmityl CoA. *Biochem. Prep.* **7**:80-3.

16- **Trievel, R. C., Wang, R., Andreson, V. E., and Thorpe, C.** (1995) Role of the Carbonyl group in thioester chain length recognition by the Medium Chain Acyl-CoA Dehydrogenase. *Biochemistry* **34**: 8597-605.

17- **Mohsen, A. A., and Vockley, J.** (1995) High-level expression of an cDNA encoding human isovaleryl-CoA dehydrogenase in *Escherichia coli*. *Gene* **160**:263-7.

18- **Powell, P. J., Lau, S., Killian, D., and Thorpe, C.** (1987) Interaction of Acyl Coenzyme A substrates and analogues with Pig kidney Medium-Chain Acyl-CoA dehydrogenase. *Biochemistry* **26**:3704-10.

19- **Kumar, N. R. and Srivastava, D. K.** (1995) Facile and restricted pathways for the dissociation of octenoyl-CoA from the medium-chain fatty acyl-CoA dehydrogenase (MCAD)-FADH2-octenoyl-CoA charge-transfer complex: energetics and mechanism of suppression of the enzyme's oxidase activity. *Biochemistry* **34**,9434-9443.

20- **Williamson, G., Engel, P. C., Mizzer, J. P., Thorpe, C., and Massey, V.** (1982) Evidence that the greening ligand in native Butyryl-CoA dehydrogenase is a CoA persulfide. *J. Biol. Chem.* **257**:4314-20.

21- **Ghisla, S. and Thorpe, C.** (2003) *Eur. J. Biochem*. submitted.

22- **Schopfer, L. M., Massey, V., Ghisla, S., and Thorpe, C.** (1988) Oxidation-reduction of general acyl-CoA dehydrogenase by the butyryl-CoA/crotonyl-CoA couple. A new investigation of the rapid reaction kinetics. *Biochemistry* **27**:6599-611.

23- **Thorpe, C., Matthews, R.G. and Williams, C.H.** (1979) Acyl-coenzyme A dehydrogenase from pig kidney. Purification and properties. *Biochemistry* **18**:331-7.

24- **Cummings, J.G., Lau, S.M., Powell, P.J. and Thorpe, C.** (1992) Reductive half-reaction in medium-chain acyl-CoA dehydrogenase: modulation of internal equilibrium by carboxymethylation of a specific methionine residue. *Biochemistry* **31**: 8523-9.

25- **Rudik, I. and Thorpe, C.** (2001) Thioester enolate stabilization in the acyl-CoA dehydrogenases: the effect of 5-deaza-flavin substitution. *Arch. Biochem. Biophys.* **392**:341-8.

26- **Vock, P., Engst, S., Eder, M., and Ghisla, S.** (1998) Substrate activation by Acyl-CoA dehydrogenase: Transition-state stabilization and p*K*s of involved functional group. *Biochemistry* **37**:1848-60.

27- **Bross, P., Andresen, B. S., Winter, V., Krautle, F., Jensen, T. G., Nandy, A., Kolvraa, S., Ghisla, S., Bolund, L., and Gregersen, N.** (1993) Co-over expression of bacterial GroESL chaperonins partly overcomes non-productive folding and tetramer assembly of E. coli-expressed human medium-chain acyl-CoA dehydrogenase (MCAD) carrying the prevalent disease-causing K304E mutation. *Biochim. Biophys. Acta*. **1182**:264-74.

28- **Saijo, T., Kim, J. J., Kuroda, Y., and Tanaka, K.** (1998) The roles of threonine-136 and glutamate-137 of human medium chain acyl-CoA dehydrogenase in FAD binding and peptide folding using site-directed mutagenesis: creation of an FAD-dependent mutant, T136D. *Arch. Biochem. Biophys.* **358**:49-57.

29- Andresen, B. S., Jensen, T. G., Bross, P., Knudsen, I., Winter, V., Kolvraa, S., Bolund, L., Ding, J. H., Chen, Y. T., Hove, V., Curtis, D., Yokota, I., Tanaka, K., Kim, J- J. P., and Gregersen, N. (1994) Disease-causing mutations in exon 11 of the medium-chain acyl-CoA dehydrogenase gene. *Am. J. Hum. Genet.* 54:975-88.

5 General Discussion

iBD over expression

For iBD over-expression in *E. coli*, several strains have been examined. The recommended strain for the pET vector used in the iBD construct is the Bl21(DE3) strain. The expression was very low and level insufficient for purification purposes. Because of the toxicity of some over-expressed proteins that affect the growth of *E. coli* and kill the expressing cells (1), especially with human genes, the C41 (DE3) strain was examined. The C41 (DE3) is a mutant of the BL21 (DE3) strain (2) and used successfully in over-expression of many proteins known to be toxic to other strains of the *E. coli* (2,3). No improvement was found for iBD over-expression in C41(DE3).

RosettaBlue^{TM}(DE3) was examined for over-expression of iBD. It contains genes responsible for production of tRNAs for the rare codons of arginine, leucine, glycine, proline and isoleucine amino acids (4). RosettaBlue^{TM}(DE3) improved iBD expression, but low activity was noticed in comparison to that expressed in the BL21 (DE3) strain. It is may be due to lack of proper folding of iBD in *E. coli* (5). An example of ACADs, which is known to have folding problems during its over-expression, is the MCAD-K304E mutant (6). MCAD-K304E requires co-expression of chaperonine GroEL/ES for proper folding when over-expressed in *E. coli*. However, this is not the rule for wild types of ACADs. My results suppose the need of bacterial chaperonine GroEL/ES to be co-expressed with cDNA for iBD in *E. coli* to improve the level of activity of expressed iBD. Vector include GroEl/ES to be over-expressed with iBD was prepared in collaboration with Prof. Vockley, MAYO Clinc, MA, USA.

Large-scale bacterial fermentations of iBD, coexpressed with GroEL/ES, were carried out in a 8-liter fermentor. About 300-400 g wet weight of cell-pastes were obtained for each fermentation process.

iBD purification

Different methods were examined for iBD purification. Phenyl Sepharose, a hydrophobic chromatography, these was abolishing enzymatic activity. The same happened with Blue Sepharose and Red Sepharose affinity chromatography.

Ammonium sulfate precipitation was found to greatly decrease the activity of iBD. Also, strong anion exchange columns, e.g. Q-Sepharose and Source Q-30 were found to be affecting the activity of iBD. On the other hand, weak anion-exchange DEAE column gave poor separation.

Presence of 5 μM of DTT, at least, found to increase enzyme stability significantly. In presence of DTT, AS and Q-Sepharose were used without any significant loss of iBD activity. DTT was thus added to all buffers used during purifications steps to increase iBD stability. Since thawing and freezing appeared to affect iBD activity glycerol was used in all buffers at a concentration of 5%.

iBD characterization

Effect of ACADs inhibitors

Different types of ACADs inhibitors examined for iBD inhibitions. Acetyl-CoA and acetoacetyl-CoA are known to inhibit ACADs enzymes (7). When examined with iBD, no inhibition found with either acetyl-CoA or acetoacetyl-CoA (the activity measured by ferrocenium assay using final concentration 15 μM of each, at 25^0C and after incubation for 10 minutes). In contrast, MCAD, for example, was inhibited by acetoacetyl-CoA (8).

Another known inhibitor for ACADs is propionyl-CoA. Previously, it was reported that propionyl-CoA cause very slow and weak inhibition of human SCAD (9). However, it is a severe and rapid inactivator with bovine SCAD (10). iBD was found to have significant activity with propionyl-CoA, amounted to be 15% that found with isobutyryl-CoA using ferrocenium assay (Fig.3, Section III).

Some ACADs are containing important cysteine residue(s) and reagent that modifying these thiol groups are known to inhibit these enzymes (9,11). iBD activity is completely inhibited by reagents that are known to affect thiol groups in proteins. Betaine (trimethylglycine) is a strong methylation reagent and known to affect thiol groups. Using 20 mM betaine, at 25^0C and after incubation for 10 minutes, was found to cause a complete inhibition of iBD. In comparison, no changes were found in the activity of human wt-MCAD when treated with betaine under the same condition. In

previous studies, rat apo-MCAD and rat apo-LCAD were severely inhibited by NEM, thiol modifying reagent, but not the holoenzymes (10). Human i3VD was 36% inhibited by NEM while rat i3VD was severely inhibited (9,11).

The results with thiol modifying reagents indicated the presence of essential cysteine residue(s) necessary for the proper structure and/or activity of iBD. This may explain the role of DTT used in purification buffers in stabilizing iBD, DTNB titrations were carried out to examine exposure of cysteine residue(s) to solvent. This method is a standard method for quantitating free sulfhydryls in proteins (12). Its mechanism of action described as follow:

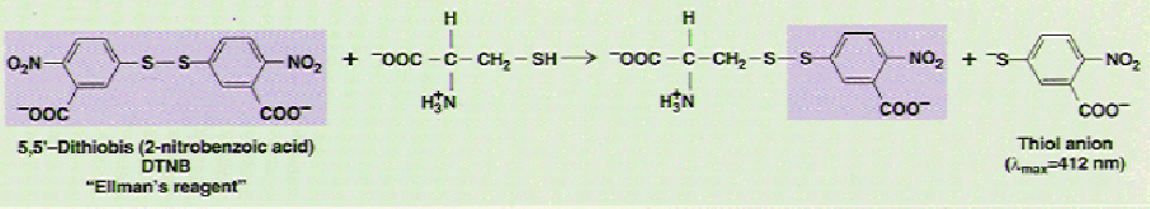

As shown before (Fig 6, Section III), the activity of iBD decreased to 50% after modification of the first 3-4 cysteine residues. The results indicate the presence of one or more cysteine residues that are exposed to solvent and are essential for iBD activity.

6 Summary

Identification and characterization of iBD and its deficiency.

Acyl-CoA dehydrogenases (ACADs) form a family of nine members that catalyze the β-oxidation of acyl-CoA substrates, they require electron transfer flavoprotein (ETF) as electron acceptor, and differ in their specificity for different types of the fatty acids linked to CoA. The ACADs can be subdivided into two subfamilies. The first comprises five members (VLCAD1, VLCAD2, LCAD, MCAD and SCAD) that catalyze the β-oxidation of "straight chain" substrates, which are degraded sequentially in the ß-oxidation cycle. The second subfamily includes four members (i3VD, i2VD, GCD and ACAD-8), which are involved in the degradation of fatty acid conjugates arising from amino acid catabolism.

In my work I have studied a previously uncharacterized protein with ACAD-like sequence (*ACAD-8*) and have defined its substrate specificity. The enzyme is an isobutyryl-CoA dehydrogenase for which the abbreviation iBD has been introduced. A single patient has previously been identified whose fibroblasts exhibit a specific defect in valine metabolism. Amplified *ACAD-8* cDNA made from patient fibroblast mRNA has a single nucleotide change (905G>A) in the *ACAD-8* coding region compared to the sequence from *ACAD-8* control cells. This encodes an Arg302Gln substitution in the full-length protein (position 280 in the mature protein), a position predicted by molecular modeling to be important in subunit interactions. The mutant enzyme was stable but was inactive when expressed in *E. coli*. It was also stable and appropriately targeted to mitochondria, but was inactive when expressed in mammalian cells.

iBD was overexpressed in *E. coli* and purified to apparent homogeneity over various chromatographic steps. Recombinant iBD is a tetramer of four subunits of molecular weight ≈42 KDa. It has a pI ≈6.2, and a maximum activity with isobutyryl-CoA (100%, K_m ≈2.6 μM), 15% with propionyl-CoA and very low activity with 2-methyl-butyryl-CoA. for isobutyryl-CoA. No activity was detected with n-butyryl-CoA and isovaleryl-CoA. iBD has sensitive SH group(s), modification of which affects the activity. The

activity pattern is consistent with the proposed role of iBD in valine degradation.

MCAD and i3VD thermal unfolding

In view of the importance of ACAD enzymes and the occurrence of genetic defects that affect stability and activity, the thermal stability of both MCAD and i3VD and of relevant mutants was investigated. The study included also the effect substrates (octanoyl-CoA and isovaleryl-CoA for MCAD and i3VD, respectively) or substrate analogues (2-azaoctanoyl-CoA and 2-azaisovaleryl-CoA for MCAD and i3VD, respectively). The K304E- and T168A-MCAD mutants that occur in genetic defects, were also studied along with A282V-i3VD mutant. The midpoint transition, T_m, for MCAD wt, K304E and T168A that reflect the protein "melting point" were 53.6, 52.6 and 47 ^{0}C, respectively, in absence of ligand. In the presence of 20 μM of octanoyl-CoA, the values were 59.7, 58.3 and 53 ^{0}C, respectively. And in the presence of 300 μM of octanoyl-CoA, the values were 63.4, 61.6 and 56 ^{0}C, respectively. With the substrate analogue, 2-azaoctanoyl-CoA, T_m for MCAD wt, K304E and T168A were 57.5, 57.3 and 49.8 ^{0}C, respectively.

In the case of wt-i3VD, T_m was 49.3 ^{0}C in absence of substrate and 55.6 ^{0}C in the presence of 20 μM isovaleryl-CoA. With the substrate analogue, 2-azaisovaleryl-CoA, T_m for i3VD wt was 47 ^{0}C. No effects were found for the T_m of i3VD-A282V mutant with or without either isovaleryl-CoA or 2-azaisovaleryl-CoA. The data indicate differences between the substrates and ligands in stabilizing MCAD and i3VD enzymes.

7 Zusammenfassung

Identifizierung und Charakterisierung von iBD

Acyl-CoA Dehydrogenasen bilden eine Proteinfamilie mit neun Mitgliedern, welche die β-Oxidation von Acyl-CoA Substraten katalysieren. Als Elektronakzeptor benötigen sie das Electron Transfer Flavoprotein (ETF). Die Enzyme unterscheiden sich bezüglich ihrer Spezifität gegenüber verschiedenen Typen von Fettsäure-CoA-Konjugate. Die Acyl-CoA Dehydrogenasen können zudem in zwei Subfamilien untergliedert werden. Die erste Subfamilie besteht aus 5 Mitgliedern (VLCAD1, VLCAD2, LCAD, MCAD, SCAD) welche die β-Oxidation von geradzahligen Fettsäuren katalysiert, die in aufeinanderfolgenden Schritten abgebaut werden. Die zweite Subfamilie beinhaltet vier Mitglieder i3VD, i2VD, iBD und GAD, die in den Abbau von Fettsäuren involviert sind, die aus dem Abbau von Aminosäuren stammen.

Ich untersuchte eine bisher nicht charakterisierte ACAD-ähnliche Sequenz (*ACAD-8*, später iBD) und definierte seine Substratspezifität. Das Enzym ist eine Isobutyryl-CoA Dehydrogenase mit der Abkürzung iBD. Die Sequenz von ACAD-8 wurde kloniert und für eine Reinigung und Charakterisierung in *E. Coli* exprimiert. Bisher wurde ein einzelner Patient identifiziert dessen Fibroblasten einen spezifischen Defekt im Metabolismus von Valin aufweisen. Die gewonnene ACAD-8 cDNA aus dem Patienten enthält einen einfachen Basenaustausch (905G>A) im Vergleich zur ACAD-8 Sequenz aus Kontrollzellen. Diese Mutation führt zu einem Austausch von Glutamin gegen Arginin an Position 302 bezogen auf das komplette Protein (Dies entspricht der Position 280 im reifen Protein). Aufgrund von Strukturanalysen wird vorhergesagt, dass diese Position wichtig für die Interaktion zwischen Untereinheiten ist. In *E. Coli* führt die Expression dieses mutierten Enzyms zu einem stabilen, aber inaktiven Protein. Das Enzym ist in Säugetierzellen ebenfalls stabil und in Mitochondrien lokalisiert, es ist aber ebenfalls inaktiv. iBD wurde in *E. Coli* exprimiert und über Q-Sepharose und Hydroxyapatit Säulen aufgereinigt. Gereinigtes iBD wurde für die Charakterisierung verwendet. iBD bildet ein Tetramer aus vier Untereinheiten mit einem Molekulargewicht von ungefähr 42 KDa. Der Isoelektrische Punkt liegt bei ≈6,2. Bei Verwendung des Ferricenium Assay hat iBD eine maximale Aktivität mit

Isobutyryl-CoA, 15% der max. Aktivität mit Propionyl-CoA. Bei Verwendung des ETF Fluoreszenz Assay liegt die Aktivität mit Isobutyryl-CoA am höchsten. Die K_m für Isobutyryl-CoA beträgt 2,6 µM. Mit n-Butyryl-CoA oder Isovaleryl-CoA wurde keine Aktivität gemessen. iBD hat Thiolgruppen, die möglicherweise entscheidend für die Aktivität und/oder Struktur sind. Dies steht im Einklang mit Ergebnissen aus Experimenten mit Thiol modifizierenden Reagenzien und deren Einfluss auf die Aktivität von iBD. Das Aktivitätsmuster bestätigt die vorgeschlagene Funktion von iBD im Abbau von Valin.

Thermische Auffaltung von MCAD und i3VD

Aufgrund der Bedeutung von ACAD Enzymen und das Auftreten von Mutationen welche die Stabilität beeinflussen habe ich den Effekt dieser Mutationen auf die thermische Stabilität von MCAD und i3VD, als Beispiele für gut bekannte ACAD Enzyme, untersucht. Diese Studien beinhalten auch den Effekt von Substraten (Octanoyl-CoA und Isovaleryl-CoA für MCAD und i3VD) oder Substratanaloga (2-Azaoctanoyl-Coa und 2-Azaisovaleryl-CoA für MCAD und i3VD) auf die thermische Stabilität von MCAD und i3VD. Zusätzlich zur Wildtyp-Form von MCAD wurden zwei Mutanten ausgewählt: MCAD(K304E) und MCAD(T168A). Zusätzlich zur Wildtyp-Form von i3VD wurde die Mutante i3VD(A282V) untersucht. Ohne Ligand beträgt die T_m (midpoint transition, Übergangmittelpunktstemperatur) für MCAD-wt, K304E und T168A 53,6°C, 52,6°C und 47°C. In Gegenwart von 20µM Octanoyl-CoA wurden Werte von 59,7°C, 58,3°C und 53°C und in Gegenwart von 300 µM Octanoyl-CoA Werte von 63,4°C, 61,6°C und 56°C ermittelt. Mit dem Substratanaloga 2-Azaoctanoyl-CoA wurde eine T_m für MCAD-wt, K304E und T168A von 57,5°C, 57,3°C und 49,8°C gemessen.

Im Falle von i3VD-wt wurde ohne Substrat eine T_m von 49,3°C und in Gegenwart von 20 µM Isovaleryl-CoA 55,6°C gemessen. Mit dem Substratanalogon Isovaleryl-CoA wurde für i3VD-wt 47°C ermittelt. Mit i3VD(A282V) konnte in An- und Abwesenheit von Isovaleryl-CoA oder 2-Azaisovaleryl-CoA keine Änderung der Tm gemessen werden. Diese Daten weisen auf die Bedeutung der Stabilisierung von MCAD und i3VD durch die Substrate hin. Diese Daten zeigen auch aufgrund der Änderungen in der T_m, dass sich die Mutationen auf die Struktur und Stabilität der Enzyme auswirken.

8 References

1- **Dohertly, A. J., Connolly, R. E., and Rothfield, L. I.** (1993) Overproduction of the toxic protein bovine pancreatic Dnase I in *E. coli* using a tightly controlled T7 promoter based vector. *Gene* **136**:337-40.

2- **Miroux, B., and Walker, J. E.** (1996) Over-production of proteins in Escherichia coli: mutant hosts that allow synthesis of some membrane proteins and globular proteins at high levels. *J. Mol. Biol.* **260**:289-98.

3- **Arechaga, I., Miroux, B., Karrasch, S., Huijbregts, R., Kruijff, B., Runswick, M. J., and Walker, J. E.** (2000) Characterization of new intracellular membranes in *E. coli* accompying large scale over-production of the β subunit of F1F0 ATP synthase. *FEBS letters* **482**:215-9.

4- **Novy, R., Drott, D., Yaeger, K., and Mierendorf, R.** (2001) *inNovations* **12**:1-3.

5- **Goloubinoff, P., Gatenby, A. A., and Lorimer, G. H.** (1989) GroE heat-shock proteins promote assembly of foreign prokaryotic ribulose bisphosphate carboxylase oligomers in *E. coli*. *Nature* **337**:44-7.

6- **Bross, P., Andresen, B. S., Winter, V., Krautle, F., Jensen, T. G., Nandy, A., Kolvraa, S., Ghisla, S., Bolund, L., and Gregersen, N.** (1993) Co-over expression of bacterial GroESL chaperonins partly overcomes non-productive folding and tetramer assembly of *E. coli*-expressed human medium-chain acyl-CoA dehydrogenase (MCAD) carrying the prevalent disease-causing K304E mutation. *Biochim. Biophys. Acta.* **1182**:264-74.

7- **Schmidt, J., Reinch, J., and McFarland, J. T.** (1981) Mechanistic studies on fatty acyl-CoA dehydrogenase. *J. Biol. Chem.* **256**:11667-70.

8- **Engel, P. C., and Massey, V.** (1971) Green butyryl-CoA dehydrogenase, an enzyme-acyl-coenzyme A complex. *Biochem. J.* 1**25**:889-74.

9- **Finocchiaro, G., Ito, M., and Tanaka, K.** (1987) Purification and characterization of short chain acyl-CoA, medium chain acyl-CoA and isovaleryl-CoA dehydrogenases from human liver. *J. Biol. Chem.* **262**:7982-7989.

10- **Okamura-Ikeda, K., Ikeda, Y., and Tanaka, K.** (1985) An essential cysteine residue located in the vicinity of the FAD-binding site in short-chain, medium-chain, and long-chain acyl-CoA dehydrogenases from rat liver mitochondria. *J. Biol. Chem.* **260**:1338-45.

11- **Ikeda, Y., and Tanaka, K.** (1983) Purification and characterization of isovaleryl-Coenzyme A dehydrogenase from rat liver mitochondria. *J. Biol. Chem*. **258**:1077-85.

12- **Wright, K. S., and Viola, R. E.** (1998) Evaluation of methods for the quantitation of cysteines in proteins. *Anal. Biochem.* **265**:8-14.

Acknowledgment

I would like to express my deep appreciation and thanks to

Prof. Sandro Ghisla, for his supervision and for his patience.

I would like also to thank

Prof. Peter Macheroux, Technical University of Granz, Austria,

Dr. Al-Walid Mohsen, MAYO Clinic, MN, USA,

Dr. Ilian Jelesarov, Zurich University, Swisserland,

Also, I thank my colleagues:

Mrs Susanne Feindler-Boeckh and Mr Robert Gradinaru.

I deeply thank My Mother, My Brothers, My Wife and My little son, Mahmoud.

Dedication

I dedicate my thesis to the Soul of My Father.